Transport Protein for Paclitaxel

A Major Qualifying Project

Submitted to the Faculty of Worcester Polytechnic Institute
in partial fulfillment of the requirements for the Degree in Bachelor of Science
in
Chemical Engineering
By

_____

Huilin Yang

_____

Mariana Harley

Date: 04/27/17

Sponsoring Organization: NSF

Project Advisors:

_____

Professor Susan Roberts, Advisor

Abstract

In this Major Qualifying Project (MQP), the transport mechanism in *Taxus* cell culture was investigated with the intent to optimize the downstream process of paclitaxel production. Bioinformatics analysis, inhibitor testing and investigation of an alternative method of paclitaxel quantification were conducted as part of the research. A homolog to the mammalian MDR protein in *Taxus* cells was identified for its potential to transport paclitaxel in *Taxus* cells. The transport mechanism was also studied using transport protein inhibitors, and results show that the concentration of verapamil affects the direction of paclitaxel transport. To simplify the investigation process, Uv-vis spectroscopy was studied as a potential substitution for UPLC to quantify paclitaxel; however, since Gamborg B5, a standard component in cell media, interferes with the assay, Uv-vis spectroscopy cannot be used as a quantification substitution. Future studies based on the investigation routes in this project can be conducted to maximizing the concentration of paclitaxel in the media via extracellular secretion and simplifying steps in the paclitaxel separation and purification process.

1. Background

1.1 Introduction of Paclitaxel

Paclitaxel (Taxol™) is a specialized metabolite, produced by the Pacific Yew tree, *Taxus brevifolia*, and largely stored in the tree bark (1). Paclitaxel is a FDA approved anticancer drug that has been widely used in different cancer treatments.

Paclitaxel induces cellular apoptosis by acting as a microtubule-stabilizing agent. Studies have found that paclitaxel can interact with the beta subunit of tubulin, which prevents the disassembly of microtubules (2). When paclitaxel is present in the cells, chromosomes are unable to separate during mitosis in metaphase, forcing the cells to enter the stage of mitotic arrest and triggering apoptosis. Unlike other chemotherapeutic drugs that inhibit microtubule assembly, paclitaxel induces defects in mitotic spindle assemble, chromosome segregation and cell division (4,5,6,7). This cell killing mechanism makes paclitaxel unique among chemotherapeutic agents.

Paclitaxel is used to treat breast, ovarian, lung, bladder, prostate, melanoma, esophageal and other types of cancers and tumors (3). It is given through an injection or infusion into the vein (Intravenous, IV). In other delivery strategies, paclitaxel is combined with a protein called albumin;

this combination is used to treat breast cancer and pancreatic cancer that has spread. The market name of this drug combination is “Abraxame” and it has proven to have reduced side effects on patients (8).

Paclitaxel by itself as a chemotherapy agent and as a pill used in combination with proteins has shown to be an effective method of treating different types of cancer. Cancer is a disease that the National Cancer Institute estimates will have 1,685,210 new cases in 2016. The fact that the disease affects such a high percentage of the world’s population indicates that the demand for anti-cancer agents such as paclitaxel is going to increase as its effectiveness against other cancers are uncovered. Full optimization of the drug production will highly benefit future patients due to market availability of the product.

1.2 Chemical structure

The chemical name of paclitaxel is 5β, 20-epoxy-1,2α,4, 7β,10β,13α-hexahydroxytax-11-en-9-one4, 10-diacetate 2-benzoate 13-ester with (2R,3S)-N-benzoyl-3-phenylisoserine. It is a complex diterpene with a taxane ring system linked to a four-membered oxetane ring at positions C4 and C5 and an ester side chain at C13 (Figure 1). Paclitaxel chemical formula is $C_{47}H_{51}O_{14}$, and its molecular weight is 853.906g/mol. It is a stable compound incompatible with strong oxidizing agents and combustibles. The melting point of paclitaxel is 213-216 °C (9).

Due to the multiple hydrocarbon rings in the structure, paclitaxel is a hydrophobic molecule. It can be dissolved in the organic solvents, such as methanol, DMSO and acetonitrile, but is insoluble in water (10). The solubility of paclitaxel in methanol is 50 mg/mL (11). Due to its hydrophobicity, paclitaxel can diffuse through the lipid bilayer membranes from extracellular to intercellular compartments in the mammalian cells (12). However, in the plant cells, beside the diffusion, studies had indicated paclitaxel is in part transported by a specific mechanism such as a channel membrane protein or a cell surface receptor. Further detail studies have to be done in order to fully understand the paclitaxel transport system (40).

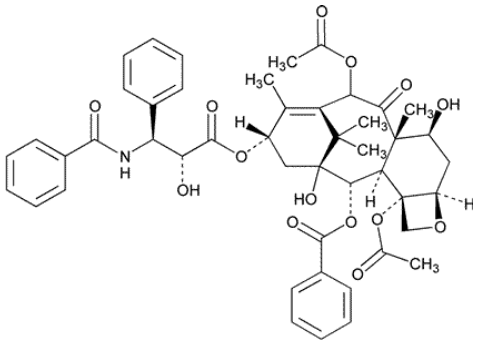

Figure 1: Paclitaxel Organic Structure (D) (13)

1.3 History of discovery of paclitaxel

Paclitaxel was discovered in 1962, through the National Cancer Institute (NCI) plant-screening program explain the goal of this screening (1), As a result of this screening, paclitaxel was found to be cytotoxic and investigators were able to isolate the active ingredients from the crude extract of the bark of the tree. Later experiments reported that the molecule had antitumor activity (14).

In 1971 Dr. Horwitz at the Albert Einstein College of Medicine in the Bronx, New York concluded that paclitaxel is able to completely inhibit the division of exponentially growing cells at low drug concentrations without interfering with DNA or RNA. In this study, the drug was found to prevent cell growth by interfering with mitosis (2), as described above.

Paclitaxel was further used as an anti-cancer treatment in clinical trials; however progress was severely limited by the shortage of paclitaxel. The high demand of paclitaxel spurred further investigation into sustainable production methods. Historically, paclitaxel has been successfully produced by four different methods, three of which are not currently used due to their complexity along with and negative social and environmental impacts. Table 1 summarizes the advantages and disadvantages of all of the production methods.

Production Method	Advantages	Disadvantages
Crude Bark Extraction	• Easiest method to extract paclitaxel • No need of harsh solvents • No expensive machinery needed for extraction	• Environmentally unfriendly • Low yield • Not year-long production
Total Organic Synthesis	• Environmentally friendly • Year-round production	• Use of harsh solvents • Just 2% percent paclitaxel yield • Many steps
Semi-Organic Synthesis	• Precursors can be extracted without killing the tree • Year-round production	• Use of harsh solvents • Low percent paclitaxel yield • Many steps • Need extraction of precursors
Plant Cell Culture	• No use of harsh solvents • Higher yield percent • Relatively cheap components for medium • No high land requirements • Manipulated system • Economically friendly • Environmentally friendly • Year-round production	• Not fully • Unknown biosynthesis pathway • Not every cell in culture is producing paclitaxel • Not fully understood Paclitaxel transport mechanism

Table 1. The advantages and disadvantages of paclitaxel production methods

1.4 Paclitaxel production methods

1.4.1 Crude extraction as a paclitaxel production method

Crude extraction has been done on the bark of the yew trees. Paclitaxel has been extracted from the bark and needles of various yew species by ordinary solvent extraction (OSE) (15). This extraction works by partially removing a substance from a solution or mixture by dissolving it in another immiscible solvent in which it is more soluble (16). The majority of OSE processes reported to use methanol as the extraction solvent at room temperature.

Many issues are associated with crude extraction method. First, the growth cycle of yew tree is long and the tree also rarely exceeds 60 cm (24 in) in diameter and 15 m (49 ft) in (17). Studies indicate that the tree should be around 100 years old to be fully ready for paclitaxel extraction. Therefore, the production via crude extraction has a high land requirement for the growth of the trees with very low yields (18).

Moreover, crude extraction is extremely environmentally unfriendly, because the bark stripping process requires sacrifice of the tree. For example, in the first conducted clinical trial, the NCI acquired *27,700* kg (60,000 lb) of dried Pacific Yew bark. However, from the *27,700* kg of dried bark, only *4* kg (9 lb) of dry and crystalline paclitaxel was extracted (19). The total amount of extracted paclitaxel was not even enough to complete the first phase of the clinical trials. This unusable low yield of the paclitaxel makes the crude extraction an environmental and economically unfeasible production method.

It is important to highlight that the bark of three mature 100-year-old trees provides only 1 gram of paclitaxel, and the amount needed for a course of the treatment of one patient is 2 grams (20). The shortage of paclitaxel from natural harvest led researchers to investigate alternative production pathways for the drug.

14.2 Total synthesis of paclitaxel

Another way of producing paclitaxel is through total organic synthesis. There have been numerous attempts to synthesis the drug. Thirty different groups and labs were working on the synthetic process, however most of them fell short due to paclitaxel's complex structure. Until 1994, Nicolaou and his group from UC San Diego and The Scripps Research Institute, and Holton and his group from Florida State University, independently published the first total syntheses of paclitaxel using different starting compounds (21, 22).

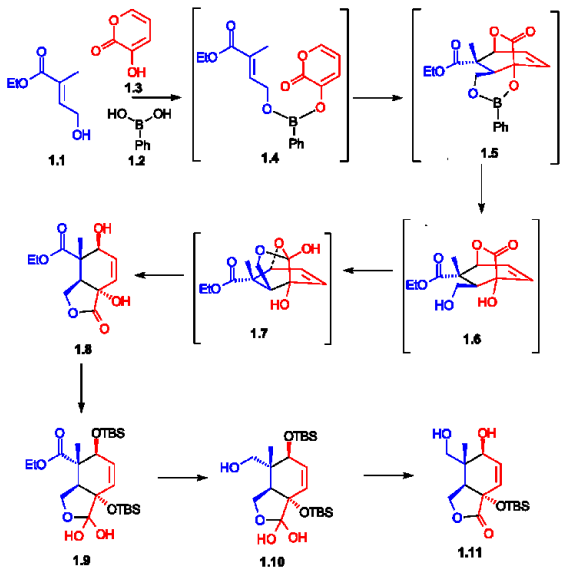

Figure 2. Nicolaus semi-sythensis C ring creation (23)

Figure 2 represents the ring synthesis steps of creating paclitaxel by the synthesis of ring C published used by Nicolaou's group. Nicolaou's synthesis was considered convergent since the final molecule is assembled from 3- preassemble synthons. Cyclohexene ring C is one of the two major parts of his synthesis. Even though total synthesis is possible, the complexity of the structure requires multiple synthesizing steps, toxic and harsh chemicals. In addition, the overall paclitaxel yield from total synthesis is low. These factors make the total syntheses production methods not economically to provide for the large scale-pharmaceutical demand.

1.4.3 Semi-synthesis of paclitaxel

The semi-synthesis method was the sole large-scale industrial method for some time. It was found that the Pacific Yew tree contained a wide range of diterpenoid derivative taxanes, which are structurally similar to paclitaxel. Paclitaxel is a member of a small group of compounds possessing a four membered oxetane ring and a complex ester side-chain in their structure, both of which are essential for antitumor activity. The amount of other paclitaxel precursors that can be extracted from the tree through the bark or needles is considerably higher than paclitaxel. Every part of the Pacific Yew tree contains much more baccatin III, 10-deacetyltaxol, 10-deacetylbaccatin III, cephalomannine and 10-deacetylcephalomannine. Therefore, it is much more promising to produce paclitaxel using these more ubiquitous precursors, since they can be recovered from collecting only needles. Baccatin III and 10-deacetylbaccatin III (Figure 3) have been extracted and used as precursors from which to initiate paclitaxel synthesis in the laboratory. They have been efficiently transformed into paclitaxel though chemical semi-synthesis (24). The semi-synthesis process requires harsh solvents and reactions, again leading investigators to find more sustainable alternative production methods.

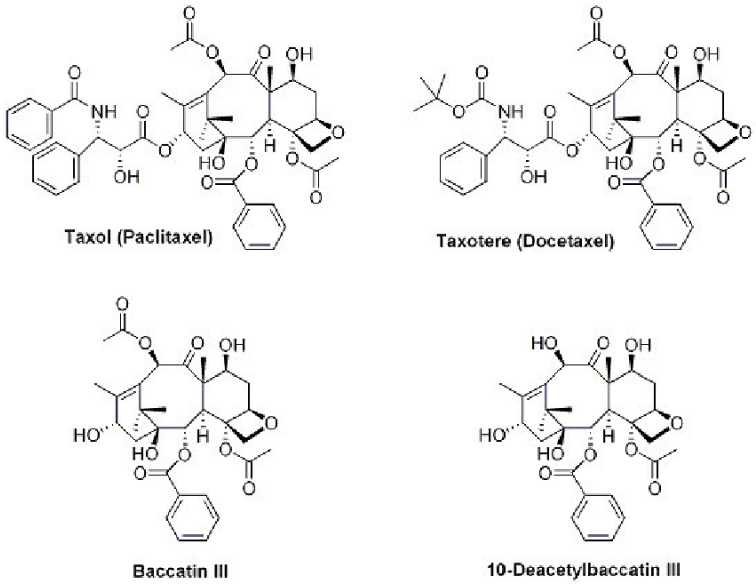

Figure 3. Baccatin III and 10-deacetylbaccatin III precursor for paclitaxel semi-synthesis (25)

1.4.4 Plant cell culture

Although the semi-synthesis method of paclitaxel was used in the industry, plant cell culture is currently the main production method of paclitaxel (26). Bristol-Myers Squibb (BMS) patented the commercialization of the compound and introduced it to the market as Taxol™. They held the contract to harvest the bark; however due through their partnership with the company Phyton (Germany) they now produce paclitaxel solely using the plant cell culture process the company developed. Current paclitaxel production comes from multiple sources, since even though BMS held the original paclitaxel license, now there are multiple generic producers (27).

Plant cell culture is preferred in the industry because it is a continuous, sustainable and high yielding method. As mentioned previously, the growth rate of yew tree is slow and the crude extraction requires sacrificing trees due to bark stripping. Comparing with the synthetic methods, plant culture uses more mild chemicals and the process is more environmentally friendly. In plant cell culture, there is also less chance of harboring human pathogens and producing endotoxins (28).

Even though the method of plant cell culture is preferred and currently used to supply paclitaxel commercially, there are many knowledge gaps that exist in the process. Much more scientific research is needed to understand and optimize the production process of paclitaxel. Currently most paclitaxel producing cell lines have been demonstrated to release as little as 7–

10% of the total paclitaxel produced to the extracellular medium (29). Further studies have suggested that most of the paclitaxel is bound to the cell walls and therefore remains associated with the cell. The lack of release of paclitaxel to the extracellular medium requires that a complex purification process is needed to obtain high yield of paclitaxel from culture. The separation process includes the steps such as product removal from media and/or culture broth, isolation using an organic solvent, crude purification and final purification.

	Cell culture	**Disruption/ Filtration**	**LLE**	**Evaporation-crystallization**	**Chromatography**
Equipment/ Supplies	Bioreactor, cells, nutrients, oxygen	Physical agitator or sonicator	Extraction unit, solvent	Vacuum crystallizer	Normal phase or reversed-phase column, solvent
Major Costs	Sterilization, equipment	Filtration equipment, energy	Solvent recovery and make-up	Equipment, energy	Equipment, labor, solvent
Fractional recovery	N/A	85-95%	80-90%	75-90%	75-85%
Purity weight	0.001-0.04%	0.1-0.5%	1-4%	60-75%	98.5-99.5%

Table 2. sequence of process steps for paclitaxel separation at large-scale (30)

Specific steps that are needed for a large-scale separation of paclitaxel are shown in Table 2. Multiple steps are needed to achieve a high recovery of paclitaxel. However, the number of purification steps can be reduced through a better understanding of the production and transport mechanism of paclitaxel in *Taxus* cultures. In other words, paclitaxel production can be optimized by further investigating the biosynthesis pathway of paclitaxel, also studying its transport mechanism to extracellular compartment and its distribution in the media.

2. Introduction of the Major Qualifying Project

The purpose of this Major Qualifying Project (MQP) is to study the transport mechanism of paclitaxel in *Taxus* cell culture with the intent to optimize the downstream process of paclitaxel recovery and purification. Particularly, the ultimate goal of this research is to maximize the concentration of paclitaxel in the media via extracellular secretion to eliminate steps in the production process.

This MQP consists of three sections: bioinformatics analysis, inhibitor testing and development of an alternative quantification method for paclitaxel. In the first section, the objective was to identify a homolog to the mammalian MDR protein in *Taxus* cells. A protein

candidate, E6Y0T0, was identified. However, its expression in the current *Taxus* cell lines and under paclitaxel producing conditions needs further study. In the second section, the objective was to study the transport mechanism through the use of transport protein inhibitors. Four different inhibitors were used and experimental results show that the concentration of verapamil affects the direction of paclitaxel transport. Finally, the third objective of this project was to develop an alternative method of quantifying paclitaxel to simplify this investigation process. Uv-vis spectroscopy was investigated as a potential substitution; however, Gamborg B5 in the media was identified as an interfering compound in the Uv-vis assay complicating quantification and necessitating the use of Ultra High Performance Liquid Chromatography (UPLC) in paclitaxel quantification

3. Methodology and experimental setup

3.1 Bioinformatics analysis

3.1.1 Literature reviews

Although the paclitaxel transport mechanism is not yet fully understood, research has provided information on specialized metabolite transport in both mammalian and plant systems. In mammalian cells, one group of proteins called multidrug resistant (MDR) proteins is responsible for anti-cancer drug efflux. This group of proteins belongs to the B subfamily of the ATP binding cassette (ABC) proteins. ABCB1 (MDR1) is the best studied protein in the group (31). MDR proteins are responsible for the extracellular transport of hydrophobic chemotherapeutic drugs in mammalian cells. Overexpression of these transporters is one of the drug resistance mechanisms used by cancer cells (31, 32). Therefore, the genetic sequences, structures and transport mechanisms of MDR proteins are well characterized. The crystal structure of ABCB1, which is known to transport paclitaxel as a substrate in mammalian cells, has been determined (33, 34) (Figure 4).

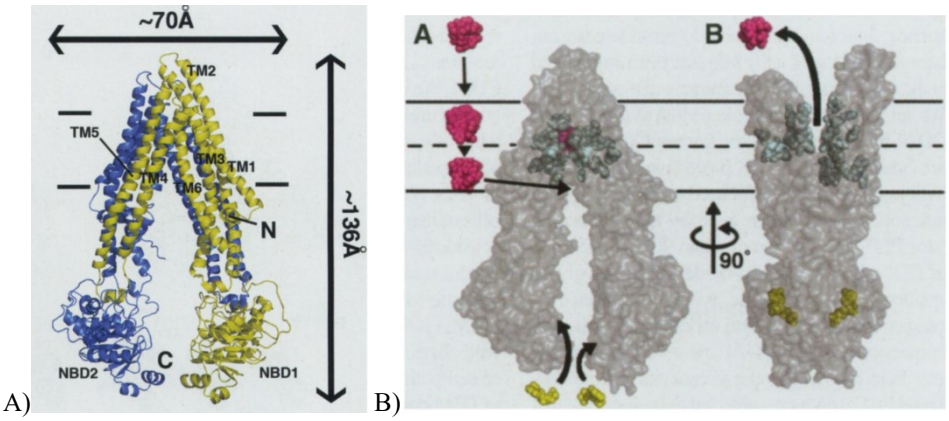

Figure 4. A. Crystal structure of ABCB1 protein; B. Proposed transport mechanism of ABCB1 (34)

An example of well-studied plant specialized metabolite transporter is a MDR-type protein, CjMDR1, in C*optis japonica*. It is responsible for uptake of berberine, a specialized metabolite, into rhizome cells. Similar to the MDR protein in mammalian cells, CjMDR1 is located in the plasma membrane (35). The proposed structure and transport function of CjMDR1 has been suggested (Figure 5). Its transport mechanism has been studied by using potential inhibitors to suppress the function of transport protein and correlation with berberine concentrations in different compartments. The gene was cloned using homology-based RT-PCR, and the function of the CjMDR1 was then characterized by transforming the genes into *Xenopus* oocytes (36, 37).

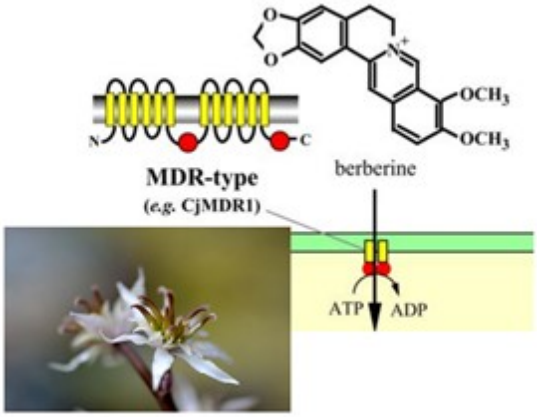

Figure 5. Proposed structure and transport function of CjMDR1 protein and a picture of C*optis japonica* (35).

Both cases above demonstrate that MDR proteins are responsible for specialized metabolite transport in mammalian and plant systems. The sequences and functions of ABC proteins are highly conserved across a wide range of eukaryote species (38). Therefore, it is hypothesized that

a MDR-type protein in *Taxus* is responsible for paclitaxel transport. Past research suggests that a specific active transport mechanism exists in *Taxus* cells since the paclitaxel can be transported against a concentration gradient and this process is dependent on calcium ion concentration (39, 40).

3.1.2 Identification of the homolog protein in *Taxus* cells

Research has shown that ABCB1 and ABCB4 MDR proteins are responsible for paclitaxel efflux in mammalian cells (41). The protein sequences of these two proteins were obtained from the National Center for Biotechnology Information (NCBI) database. Since the function of a protein is determined by its protein sequence, the protein sequence of a protein with homologous function in *Taxus* should be similar to that of MDR proteins in mammalian cells. In order to identify a protein with high similarity to the known MDR proteins in mammalian cells, the database was searched against the known sequences of ABCB1 and ABCB4. Protein sequences are considered identical if aligning amino acids in the sequences are exactly the same. When corresponding amino acids in the sequences are not the same but have similar chemical properties, such as leucine and valine, the sequences are considered similar to each other (42). The more identical or similar amino acids exist in the sequence of interest, the higher percentage of identity or similarity of that sequence comparing with the known sequences. The generally accepted rule is that two sequences need to have at least 30% identity to be considered as homologs (43). Therefore, the search results were sieved with a 30% identity threshold to be considered as homologs. Once a protein candidate was identified from the *Taxus* transcriptome (available in the Roberts laboratory), its protein sequence was aligned with the sequences of known MDR proteins on the NCBI website by using the align function. The similarity and identity of the sequences in the functional domains were also obtained from the website to further confirm the similar function of the MDR protein and the protein candidate. The complete proteins sequences and alignments are included in Appendix A and B.

3.1.3 Confirmation of the protein candidate existence in *Taxus* cell cultures

After identifying the protein candidate in the database, the existence of the protein candidate sequence in the genome of current *Taxus* cell cultures maintained in the Roberts laboratory was studied via polymerase chain reaction (PCR) on the DNA extracts of all the *Taxus* cell lines available. The goal was to amplify the gene through PCR and visualize a band through

gel electrophoresis of the expected length; these data would suggest the gene sequence was present in the genome of the cell lines. Because the *Taxus* genome has not yet been sequenced, only the transcriptomic data of E6Y0T0 was available (included in Appendix C); therefore, primers were designed based on the mRNA sequence of the protein candidate from the NCBI Primer-Blast website. A PCR product size in the range of 3000 to 4500 bp was expected because the length of the mRNA is about 3900 bp. The minimum, maximum and optimum primer melting temperatures were set to 57 °C, 63 °C and 60 °C respectively. Ten pairs of primers were designed. The melting temperature, possibility of self-dimerization and hairpin formation, and Gibbs free energy of the primers were considered through assistance of the Technical Support Department of Integrated DNA Technologies (IDT). Primers that can be used in the PCR reaction should have melting point below 65 °C, low possibility of formation self-dimerization and hairpin, and Gibbs Free Energy no negative than -9 kcal/mol (44). The pair of primer that best fits these requirements was suggested by the Technical Support Department, which is, was used for the PCR experiment. The time and temperature cycle of the reaction in the thermo cycler was set as shown in Figure 6.

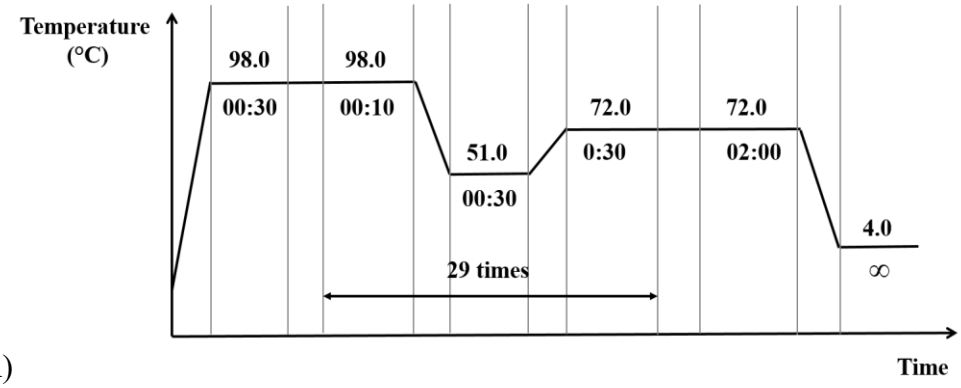

A)

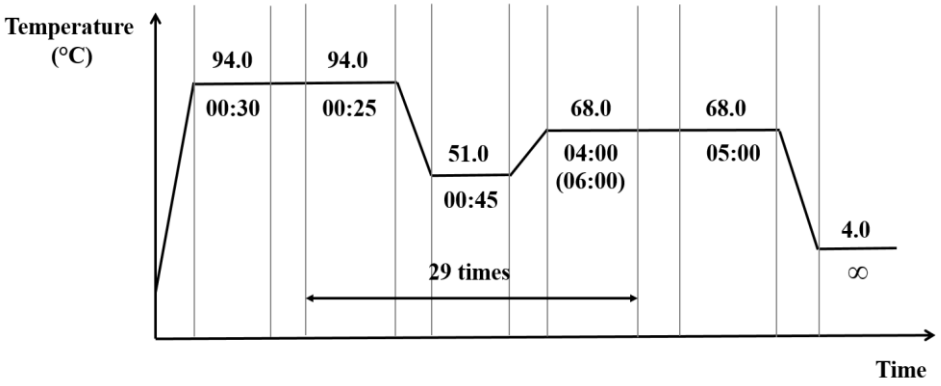

B)

Figure 6. The thermocycles of PCR reactions using A) Taq and B) Q5 polymerase

Two different DNA polymerases, Q5 and Taq, were used in the reaction. Although Taq is one of the most common DNA polymerases used, Q5 is a more robust DNA polymerase since it has about 280 times higher fidelity than Taq. In other words, the amplicons will be more accurate when Q5 is used in the PCR (45, 46). To ensure the target gene could be amplified and the gene identification in the cells would not be influenced by the robustness of DNA polymerase, both Q5 and Taq were tested. Two extension times, 4 min and 6 min, were used to make sure the gene was fully amplified despite the long product length. DNA extraction of *Taxus* cell lines P93AF, C093D, P093XC and 21260C, and *Arabidopsis* cells (as a negative control) was performed following the instructions of the DNeasy® Plant Mini Kit from Qiagen. Among these cells lines, only 21260C is currently accumulating paclitaxel. *Arabidopsis,* one of the model organisms for plant research, was used as a negative control in the test. Agarose electrophoresis was used to visualize the PCR product. Agarose gels were made and used along with the DNA ladder O'RangeRuler 200 bp from Thermo Scientific to confirm the band size. SYBR Safe, a DNA gel stain from Thermo Fisher Scientific, was added to the gels for DNA visualization. The gels were run at 110 volts for 40 minutes. The results were captured under UV light.

3.2 Inhibition of active transport

3.2.1 Literature review: inhibitors selection

To better understand MDR proteins, the cancer researchers have studied inhibition of the transport mechanism to develop a solution for drug resistance. Verapamil has been identified as an inhibitor for ABCB1 and other MDR proteins for its activity as a calcium pump blocker (47). It has been used block the efflux of paclitaxel in mammalian cells (39). The binding sites of verapamil in ABCB1 have been identified as Leucine (Leu) 65, Isoleucine (Ile) 306, Isoleucine (Ile) 340, and Phenylalanine (Phe) 343 (shown in Figure 7).

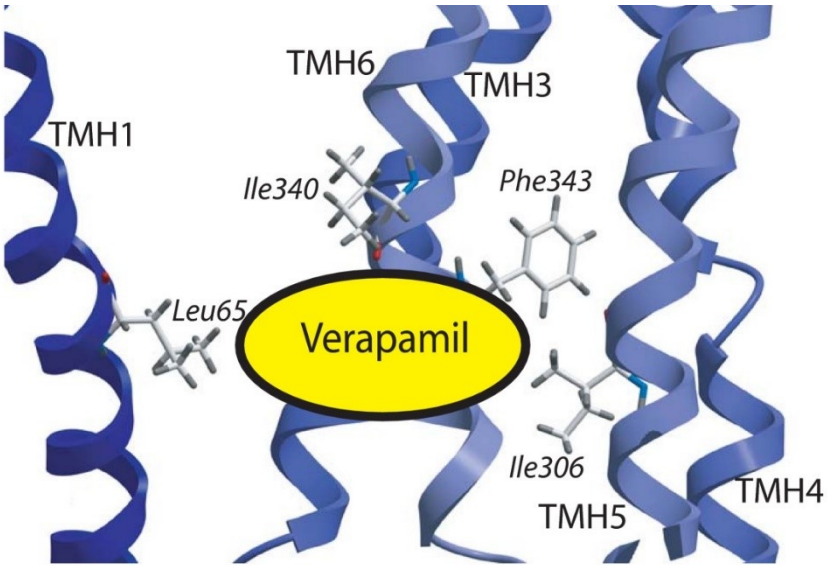

Figure 7. The binding site of verapamil in ABCB1 protein (38).

Since verapamil inhibits paclitaxel efflux via MDR proteins from mammalian cells (38), it could also inhibit the transport of paclitaxel in *Taxus* cells. Similar to verapamil, cyclosporine A has also shown inhibition of transport of specialized metabolites in the studies of berberine. According to the studies, cyclosporine A can inhibit the uptake of berberine by rhizome cells (48). It is a known inhibitor for ABCB1 protein and it most likely inhibit the protein function by blocking the transport pathway (49). Therefore, it is also a good inhibitor candidate for the MDR-type transport protein in plant cells, especially in *Taxus* cells. Moreover, since the MDR proteins belong to the ABC transport protein family, the activities of MDR proteins are dependent on ATP consumption. Theoretically, the activity of the MDR proteins should be inhibited by the ATPase inhibitors although the side effects on other cellular ATP-dependent activities should be considered. Vanadate, a potent inhibitor of ATPase, therefore, may affect the paclitaxel transport mechanism of a potential MDR-type transport protein in *Taxus* cells (39). In addition to inhibitors of MDR proteins, scientists also identified inhibitors for non-MDR proteins in the ABC protein family. Genistein, an inhibitor of the proteins in ABCG subfamily, is one example (50). It could inhibit tyrosine autophosphorylation, which is used in ABCG protein action (51).

All four inhibitors mentioned were used to investigate paclitaxel transport in *Taxus* in this project. Verapamil, cyclosporine A, and vanadate were used to investigate the transport

mechanism by inhibiting the activity of the potential MDR-type protein. Genistein, however, was used as a negative control in the experiment. In other words, since it is an inhibitor of ABCG protein that does not belong to the MDR proteins family, paclitaxel transport should not be affected when genistein is used. When the Verapamil, cyclosporine A, and vanadate are incubated with *Taxus* cells individually, the concentration of the paclitaxel in the media and cells should be different than that in the cell culture without the inhibitor treatment. However, when genistein is incubated with the cells, the concentration of paclitaxel inside or outside of the cells should be comparable with the cell culture that does not have the inhibitor treatment. In general, the paclitaxel uptake was been inhibited if the concentration of paclitaxel in the media is higher in media and lower in cells with than that in the culture without the treatments. If the reverse is true, then the paclitaxel uptake was been facilitated.

3.2.2 Cell viability test in the presence of the selected inhibitors

A cell viability test with the inhibitors (verapamil, cyclosporine A, and genistein), the paclitaxel delivery solvent (methanol) and the cyclosporine A and genistein delivery solvent (DMSO) was performed to determine whether the compounds and solvents would compromise cell viability. 12.5 µl of 100 mM inhibitors solutions were added to 10 mL *Taxus* cell cultures in 25 ml flasks and incubated for 48 hours. The final concentration of the inhibitors in the cell culture was 125 µM. The viability of cells was tested twice: after 24 hours incubation and after 48 hours incubation. 1 mL of cell with media samples were taken at each time point. 10 µl of 0.5 mg/mL Fluorescent diacetate (FDA) and 5 µl of 0.1 mg/mL propidium iodide (PI) were added into each cell culture sample and used as indicators for cell viability and death respectively. If the cells are alive, non-fluorescent FDA would be converted to fluorescein with green fluorescence (52). If the cells are dead, the PI would be able to permeate the cell membranes and stain the nuclei with red fluorescence. Fluorescent microscopy was used to visualize the cells with the stains by using an absorbance at 494 nm and emission at 520 nm to identify alive cells and an absorbance of 536 nm and emission at 617 nm to identify dead cells. The culture viability was quantified by estimating the percentage of the live and dead cells through a quick visualization test.

3.2.3 Initial inhibitor test

3.2.3.1 Experimental setup

After confirming the effect of the inhibitors and solvents on the viability of cells, we tested all of the inhibitors to determine if they influence paclitaxel transport. Two final concentrations of inhibitors were added to the culture: 50 µM and 100 µM of verapamil, cyclosporine A and genistein in DMSO and 1 mM and 0.5 mM of vanadate in water. Each inhibitor solution was added to 15 mL P093X line *Taxus* cell culture at day 7 and pre-incubated for 1 hour. There are triplicates for each inhibitor treatment. Paclitaxel was then dissolved in methanol added after pre-incubation at a final concentration of 8.3 mg/L, and the volume percentage of methanol in the cell culture is about 0.3%. The cells, inhibitor, and paclitaxel were incubated and sampled at 1.5, 3, 6 and 24 hours. For each time point, 1 mL of total culture was sampled along with 1 mL of liquid media.

3.2.3.2 Sample processing for UPLC analysis

The cell and media only samples were processed to be tested via UPLC for paclitaxel quantification. The processing procedure is shown in Figure 8.

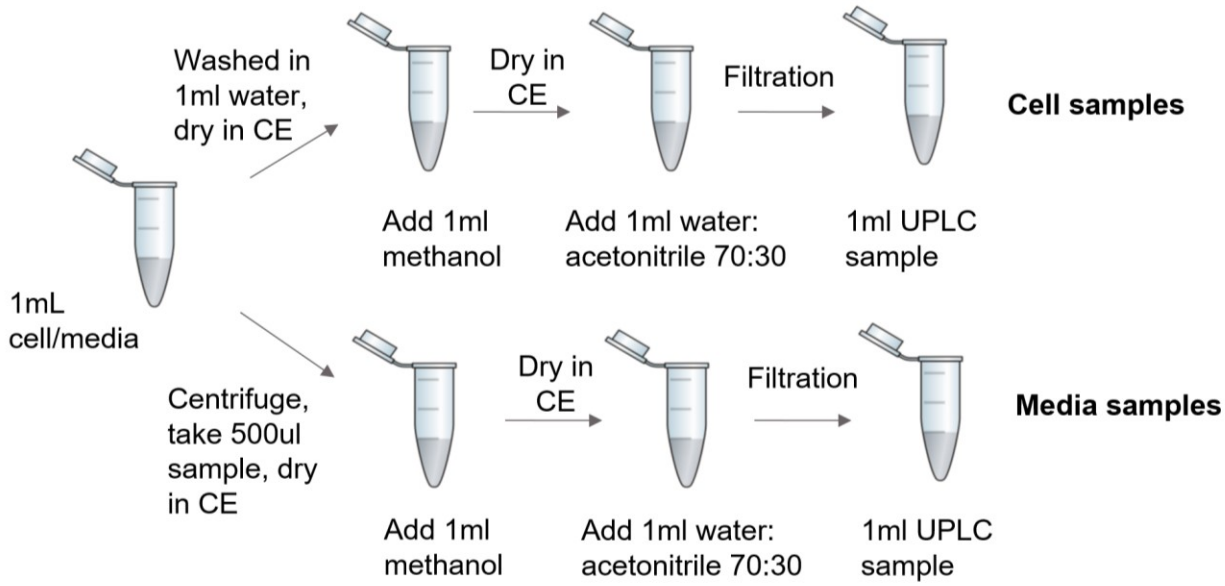

Figure 8: Inhibitor Sample Methodology. CE stands for centrifugal evaporator.

Cell samples were washed with nanopure water and the media samples were centrifuged to isolate the supernatant in 1.5 mL micro-centrifuge tube and remove all particulates. Both cell and media samples were dried in the centrifugal evaporator overnight and re-suspended in 1 mL of methanol. After being sonicated in an ice bath for 30 minutes to make sure the dry pellet was

dissolved in the methanol, the samples were centrifuged at 132,000 rpm for 20 minutes to obtain the supernatants. The supernatants were transferred to fresh 1.5 mL micro-centrifuge tubes and put into the centrifuge evaporator again for six hours. All the samples were re-suspended again in 70:30 water: acetonitrile solution. The samples were then filtered through a 0.22 μm filter directly into the UPLC glass vials. The vials were placed into the UPLC and the concentration of paclitaxel in the samples were quantified using a standard curve generated with varying levels of paclitaxel in the same UPLC run.

3.2.4 Investigation of the effect of concentration on inhibition

To further investigate the effect of inhibitor concentration on paclitaxel transport, we added verapamil to P093X *Taxus* cell cultures at a higher concentration than what was used in the previous inhibitor test. Similar to the setup of the previous test (described above), verapamil solution was added to the cell culture to achieve a final concentration of 100 μM. Verapamil was incubated with the cell cultures for 30 min and the paclitaxel solution was next added to achieve the final concentration of 50 mg/L. 1 mL media samples were taken at 5 min, 15 min, 30 min, 1 hour, 6 hours and 24 hours. The same processing procedure was used to prepare the cell and media samples for paclitaxel quantification on the UPLC, except the media samples were not centrifuged before they were dried in the centrifugal evaporator in the first step.

3.2.5 Statistical analysis

Two-way Anova and Student's t-test were used to analyze the experimental data of the inhibitor test. Two-way Anova was used for the results of the first inhibitor test. It was used since there are two independent variables in the experimental setup: the inhibitor treatments and the time. The dependent variable is the concentration of paclitaxel. The purpose of the two-way Anova was to study the interaction between the independent variables and the dependent variable. Particularly, for the inhibitor test, two-way Anova was used to study the effect of inhibitors and incubation time on the paclitaxel concentration. The test was conducted by using Graphpad software. In the test setup, data were entered so that each row represent a time point, and the concentrations of paclitaxel at each time point from the same culture were in the same column. A sample data entry for the verapamil treatment and control group is shown in Figure 9.

Table format: Grouped		Group A			Group B			Group C		
		V-50			V-100			Control		
		A:Y1	A:Y2	A:Y3	B:Y1	B:Y2	B:Y3	C:Y1	C:Y2	C:Y3
1	1.5h	0.194966	0.235375	0.216654	0.245876	0.321842	0.284059	0.354774	0.072827	0.031847
2	3h	0.220707	0.040808	0.005765	0.041721	0.074311	0.213629	0.383597	0.484390	0.240568
3	6h	0.481137	0.365390	0.360425	0.303122	0.507677	0.567605	0.410095	0.373742	0.321917
4	24h	0.412723	0.443218	0.360560	0.412836	0.410545	0.402171	0.266975	0.399429	0.295554

Figure 9. Data entry of the two-way Anova test for the test results of media samples from verapamil treated cell culture and the cell culture without inhibitor treatment. Group A, B and C represent the cell culture with 50 µl of 50µM, 100µM and nanopure water treatment. Y1, Y2 and Y3 represent three replicates of each treatment.

A two-way Anova report is generated by the software. The setup window is shown in the Figure 10.

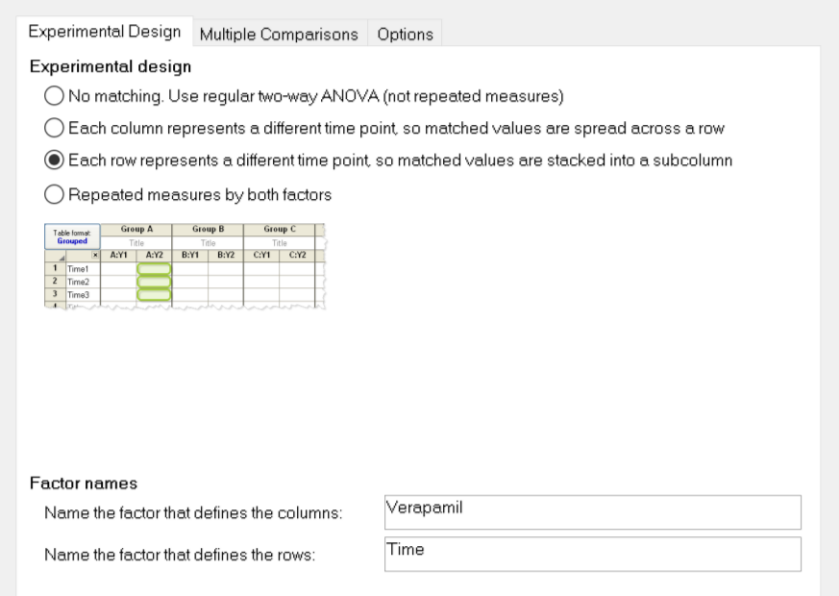

Figure 10. The setup window of a two-way Anova test in Graphpad

In the report, the statistical significance of the effect of inhibitor treatment and time were reported. In the inhibitor test results, *=p<0.0332, **=p<0.0021, ***=p<0.0002 and ****=p<0.0001 as compared to the results of cell cure without treatment.

Two-way Anova could only show the statistical significance between the variables. It cannot identify the particular interactions between the subgroups of variables that caused the statistically significant difference. For example, the test can only tell if the inhibitor treatment has significant effect on the concentration of paclitaxel, but it cannot show which concentration of inhibitor has the effect. To identify interactions within the subgroups, a Tukey's multiple

comparison test was done for each treatment with the control group. Based on the test result, it could be determined if the change in paclitaxel concentration is significant by using inhibitor. An example of the Tukey comparison setup is shown in Figure 11.

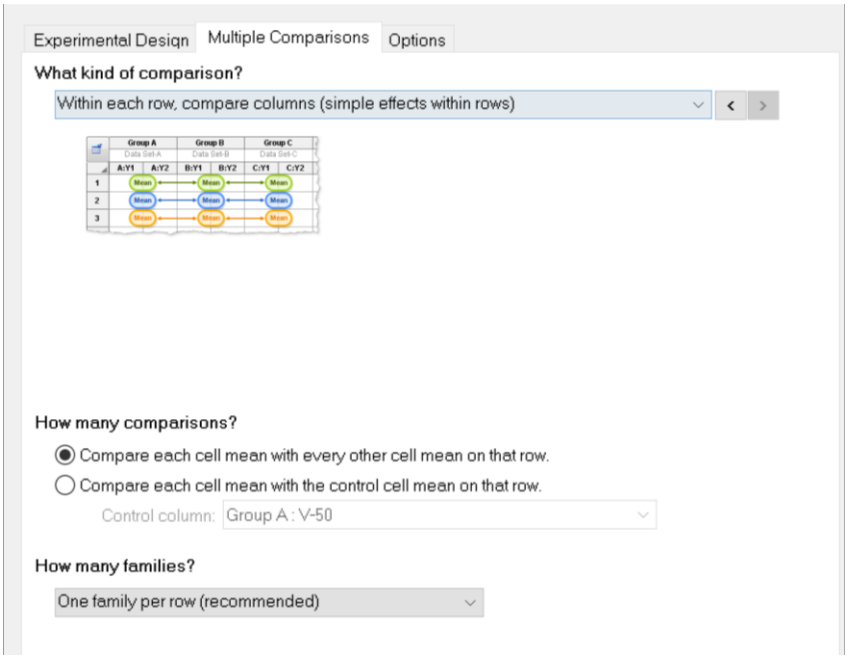

Figure 11. The setup window of a Tukey's multiple comparisons test

For the experiment result of the inhibitor test for investigating effect of inhibitor concentrations, Student's t-test was conducted for the data analysis. The t-test assumes unequal variances was used because there is only one independent variable, treatment of verapamil or not. To be able to do parallel comparison, the data of verapamil treatment group from the preliminary inhibitor test were also analyzed by the t-test. All the t-tests were conducted in Excel. In the test, a "*" indicates $p<0.05$. A sample of the t-test result is shown in Figure 12.

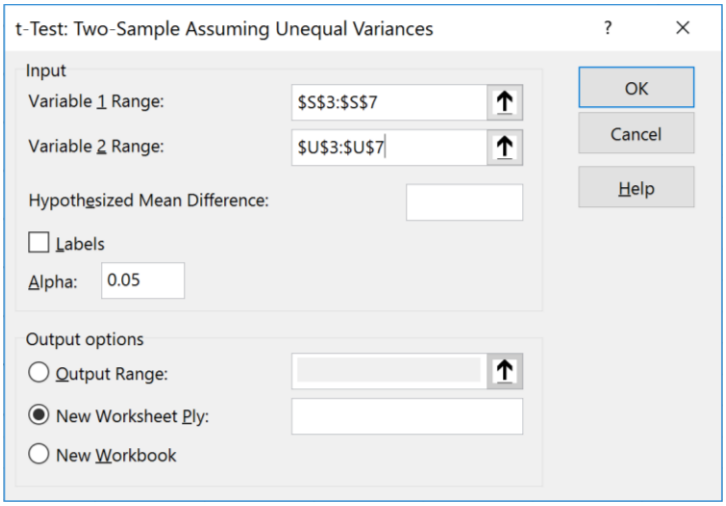

Figure 12. The setup window of a Student's t-test in Excel

3.3 Alternative method of paclitaxel quantification

3.3.1 Literature review

Concentrations of paclitaxel are typically quantified using UPLC. It is a technique that can be used to separate, identify and quantify the compound of interest in a mixture. Within the apparatus, compounds are separated by interacting differently with a column composed of solid absorbents. A pressurized liquid, also known as the "liquid phase", is used to influence the interactions and to elute the compounds from the column. The concentrations of the separated compounds are analyzed by a UV/vis detector (53). A similar detector is also used in UV-vis Spectroscopy. The detector can measure the light absorption caused by the transition of electrons from ground state to an excited state in a particular molecular structure of the compound of interest. The strength of the absorbance would indicate the concentration of the compounds (54). Since UV-vis spectroscopy also uses a UV/vis detector to quantify the concentrations of compounds, these two machines are essentially using the same principle of quantification, which is Beer's Law. Research has been done for the comparison of UV-vis spectroscopy and high performance liquid chromatography (HPLC), a less optimized version of UPLC. According to the test results, though the HPLC is more accurate than the UV-vis spectroscopy, both methods are reliable for the quantification of pharmaceutical formulations and UV-vis spectroscopy is the more economical testing option (55, 56). Therefore, in this project, UV-vis spectroscopy was hypothesized as a faster and cheaper alternative method for paclitaxel quantification.

3.3.2 Preliminary test of UPLC samples in UV-vis

The preliminary tests were done by testing UPLC samples in the UV-vis spectroscopy, using water-acetonitrile solution as a blank. Since a peak at 230 nm is used to characterize paclitaxel, all absorbances were read at that wavelength (57). A pair of quartz cuvettes was used due to the low wavelength to avoid the interference of absorbance from another cuvette. The calibration curve of absorbance against paclitaxel concentrations was made through reading water-acetonitrile samples with known paclitaxel concentrations. Since paclitaxel is added into the media instead of directly into water-acetonitrile solution, it is also necessary to obtain the standard curve for media based solution with known paclitaxel concentrations. Like the standard curve of paclitaxel in the pure water-acetonitrile solution, the standard curve for media based samples was obtained by testing a range of paclitaxel concentration from 10 mg/L to 70 mg/L. To prepare the media based samples, 1 mL media aliquots were obtained from the flasks of *Taxus* cell cultures at day 7, halfway through the cell transfer cycle, and paclitaxel-methanol solution was added to make the aliquots with different known concentrations of paclitaxel. The aliquots were dried in the centrifugal evaporator and resuspended in methanol and water-acetonitrile solutions following the identical procedure of UPLC samples processing described above. The aliquots were tested with UV-vis spectroscopy, using water-acetonitrile solution as a blank, and the absorbance at 230 nm was recorded.

3.3.3 Identification of the interfering compound

There are four main components in the media: Gamborg B5, sucrose, 6-benzylaminopurine (BA), and naphthaleneacetic acid (NAA). Based on the recipe of the media, 0.0321 g of Gamborg B5, 0.02 g of sucrose, 1.2 µl of BA, and 27 µl of NAA were dissolved in 10 mL nanopure water separately. The well mixed solutions were tested three times each with UV-vis spectroscopy using water as a blank.

4. Results and discussion

4.1 Bioinformatics analysis

4.1.1 Identification of the homolog protein in *Taxus* cells

According to the NCBI search results, a gene named E6Y0T0 in the *Taxus cuspidata* transcriptome was identified as a transport protein candidate. The protein sequence of

E6Y0T0 is 42.2% identical and 61.5% similar to that of ABCB4 (MDR3) protein, and 40.6% identical and 61.0% similar to that of ABCB1 (MDR1) protein. All the sequences are included in Appendix A and the alignment of all three sequences is included in Appendix B. Using 30% as the threshold for homolog protein identification, E6Y0T0 is considered as the homolog to the two MDR proteins in mammalian cells and therefore should have similar function as the two proteins. To support this idea, particular attention was paid to the alignment of the functional domains. As mentioned previously, MDR proteins belong to a subfamily of ABC protein. Their functional domains are, therefore, characterized as the ABC transporter domains. The alignment results are shown in Figure 13.

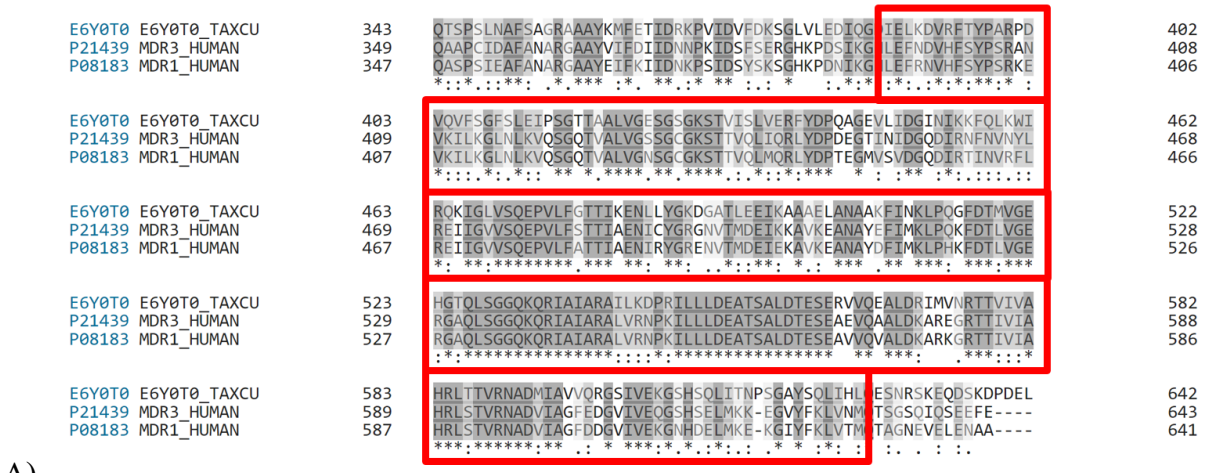

A)

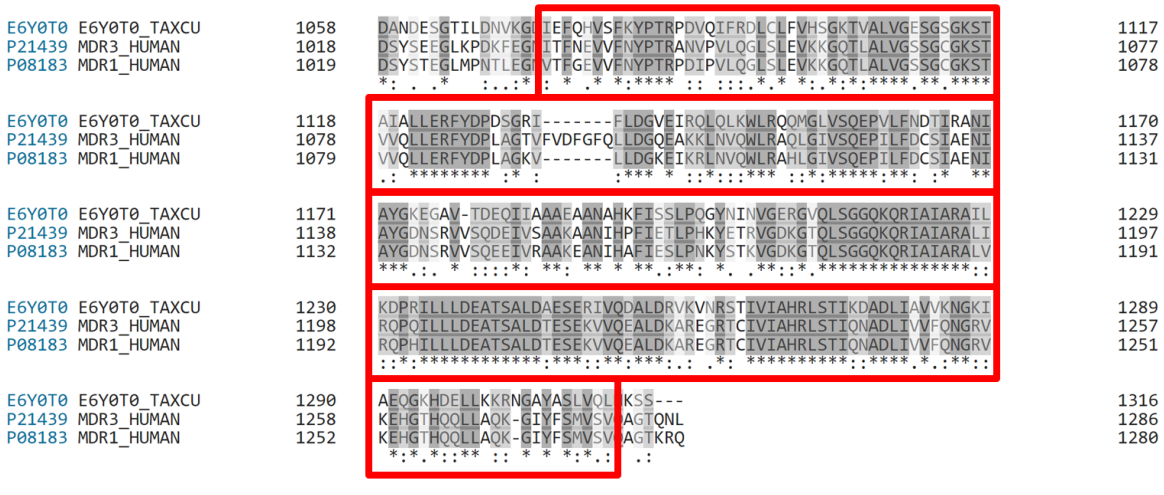

B)

Figure 13. The alignment of ABC transporter domains. A) transporter domain 1 and B) transporter domain 2. The darker gray or "*" in the figure indicate identical amino acid among the sequence, while the lighter gray or ":" and "." indicate similar amino acids

When the sequence of the three proteins are aligned together at the specific domains, E6Y0T0 has 54% identity and 88% similarity to the ABCB1 and ABCB4 sequences in the transporter domain 1 and 53% identity and 85% similarity to the ABCB1 and ABCB4 sequences in the transporter domain 2. Comparing with the identity and similarity of the entire sequence, both percentages are higher when only the sequences of functional domains are compared. Overall, since the structure and function of a protein is highly dependent on it sequence, it is highly possible that the protein candidate, E6Y0T0, has similar functions as the mammalian MDR proteins that is responsible for paclitaxel efflux.

4.1.2 Confirmation of the protein candidate in *Taxus* cell culture

To conduct PCR of E6T0Y0 in the genome of current *Taxus* cell lines, 10 pairs of primers were designed and the best pair of primers was suggested by IDT. The forward primer is 5' ACATGGCTAAGGCAAAGGACA 3' and the backward primer is 5' ACCCCCAGATAATTGCACCC 3'. PCR was done with this pair of primers and the Taq DNA polymerase. The electrophoresis gel results of the PCR reaction are shown in Figure 14.

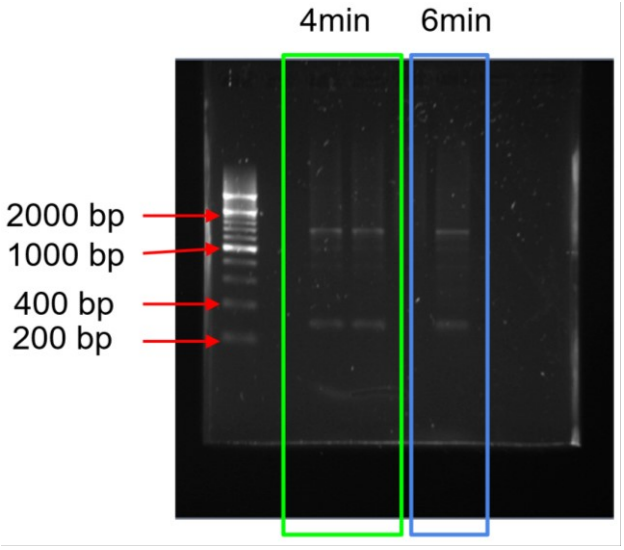

Figure 14. The electrophoresis results of PCR reactions using Taq DNA polymerase and the DNA extract of P093AF. The extension times were set to 4 min or 6 min for each PCR reaction.

There are two distinct products from each PCR reaction (Figure 14). One is approximately 1500 base pair (bp) and the other is approximately 300 bp. However, according to the mRNA sequence of E6Y0T0, the amplicons of the gene should be at least 3500 bp. There could be three

potential explanations for the smaller sizes of PCR products. First, the extension time could be too short so that the long sequence was not fully amplified during the reaction. Second, the polymerase might not be robust enough to build such an extensive sequence without falling off. Third, the primer sequence could be non-specific within the genome and random, shorter DNA segments were amplified. To test the possibility of using insufficient extension time, the PCR reaction was performed at 4 min and 6 min separately, while 6 min is two and half minutes more than the recommended extension time. However, the size of PCR products did not change when longer extension time was used (Figure 14). Therefore, the extension time was likely not the cause for the small PCR products.

To further investigate the cause of the smaller PCR products, more comprehensive experiments were conducted. A more robust DNA polymerase, Q5, was used in parallel with Taq DNA polymerase. Genomic DNA was extracted from multiple *Taxus* cell lines and one *Arabidopsis* cell line (control) and used in the PCR with the designed primers (Figure 15).

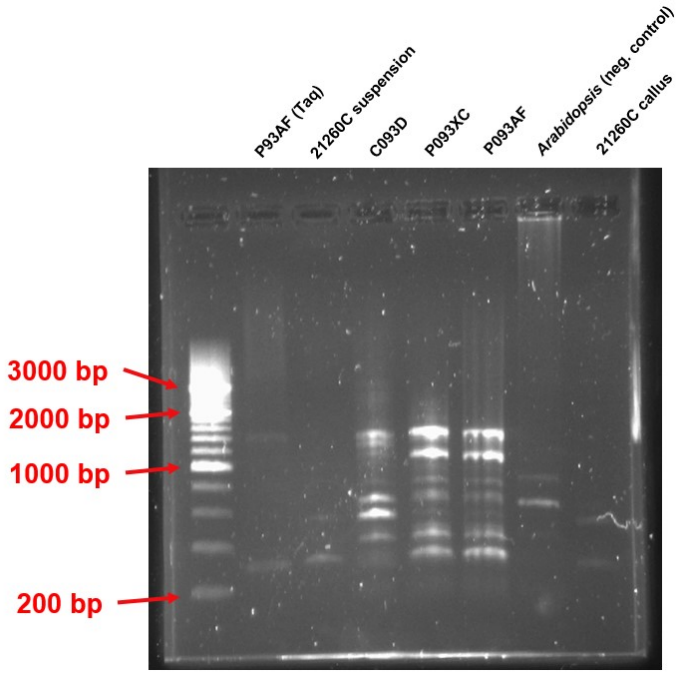

Figure 15. The electrophoresis results of PCR reactions using Taq and Q5 DNA polymerase and the DNA extract of all cell lines. Taq was used to amplified the DNA segments shown in the second lane from left to right. Q5 was used to amplify the rest of DNA segment on the gel.

Since a higher size of product will have stronger signal on the agarose gel as a brighter band, the strong signal of the products amplified by Q5 indicate it is a more robust DNA polymerase. However, all the products amplified by both DNA polymerases were smaller than

3000 bp. Thus, the smaller size of PCR reaction products is not likely caused by the low effectiveness of DNA polymerase. Moreover, the amplicons of the DNA from other *Taxus* cell lines and *Arabidopsis* cells had similar sizes, smaller than 3000 bp as well. The genomic DNA extract of *Arabidopsis* was included in this experiment as a negative control so we did not expect to see any band. A search of the primer sequences against the database of *Arabidopsis* genomic DNA sequence was performed through The *Arabidopsis* Information Resource (TAIR) prior to the experiment and no hit was found. In theory, the genomic DNA of *Arabidopsis* should not be amplified in PCR reaction. However, there were bands shown on the agarose gel, indicating DNA segments of *Arabidopsis* were amplified (Figure 15). Therefore, it is mostly likely that the primers that were used in all the reactions were non-specific. In other words, the primers can bind to undesired sections of genomic DNA in both *Taxus* and *Arabidopsis* cells. The binding affinity of the primers was strong enough for the DNA polymerase to start amplifying the undesired segments.

There could be two reasons for the non-specific primer binding. First of all, the primer was designed based on the mRNA sequence instead of the DNA sequence of the E6Y0T0 protein. Since the sequence of mRNA does not include the introns in DNA and introns are a component of eukaryotic genomes, it is highly possible that the mRNA sequence of E6Y0T0 does not fully represent the entire DNA sequence of the protein. Moreover, the continuous segments of the mRNA sequences on which the design of primers were based could be separated by introns in the DNA sequence and undergo splicing post-transcriptionally. Consequently, the primers might not be able to precisely bind with the DNA at the desired location in the *Taxus* genome.

The size of the target gene is close to the medium size of the common amplification size in the PCR reaction (0.1 to 10 kilo base pairs) (58). Since there are about 3500 bp nucleic acids that encode the protein structure in the mRNA sequence, the entire DNA sequence would be even larger when introns are considered. While the sequence is not fully known, the designated locations of primers' binding sites could be farther from each other than expected due to the large size of the target gene. It is possible to have similar binding sites in between the two designate ones, for example, in the intron areas. Therefore, the binding of the primers could be less specific.

More information about the genomic DNA sequence of this protein is needed to be able to confirm E6Y0T0 in the current cell cultures using PCR. Another alternative method would be using the technique of real time PCR (RT-PCR) to verify expression of the gene in the cell cultures.

4.2 Inhibition of active transport

4.2.1 Cell viability test with the selected inhibitors

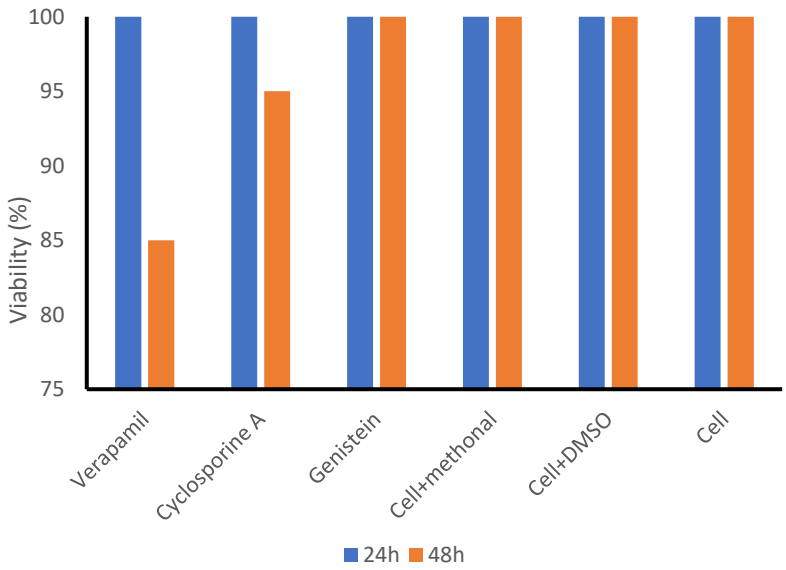

Figure 16. Cell viability test results after 24 h and 48 h incubation. P093X cell line was used.

After the first 24 hour incubation, all the cells with treatments are 100% alive (Figure 16). This is the comparable to the negative control result where cells were incubated without treatment. After the 48 hours of cells incubation, cells with verapamil, genistein and cyclosporine A showed a decrease in viability. However, the viability of the cultures was not lower than 85%. Therefore, the inhibitors, methanol, and DMSO did not have a significant effect on the viability within 48 hours of incubation and they have no effect on cell viability for the first 24 hours of incubation. Therefore, the time interval selected for the experimental procedure of the inhibitor test was 24 hours.

4.2.2 Inhibitor test

Verapamil, genistein, cyclosporine A and vanadate were used for the initial inhibitor test. For each inhibitor, two concentrations were tested. Cell culture with no addition and cells incubated with DMSO were the two controls in the experiment. All groups of cells were spiked with paclitaxel and cell culture and media samples were taken at four time points. The concentration of paclitaxel in the media or cell samples were tested in UPLC and results are shown in Figure 17. The results of statistical analysis are included Appendix D.

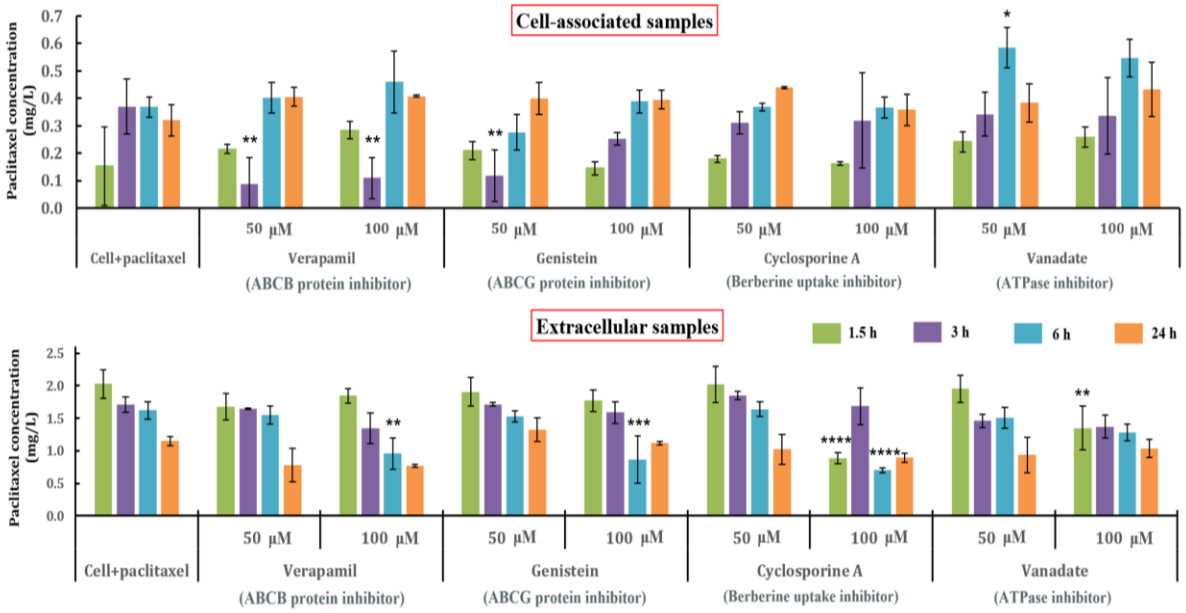

Figure 17. Results of inhibitor test: A) Paclitaxel concentration in cell-associated samples, B) Paclitaxel concentration in media samples. *=p<0.0332, **=p<0.0021, ***=p<0.0002 and ****=p<0.0001 as compare to control (cell+paclitaxel) according to two-way Anova and Tukey's multiple comparisons test, N=3. The error bars represent the standard deviation of triplicates.

In general, the paclitaxel concentrations in the cell samples increased over time, while the paclitaxel concentration in the media samples decreased over time. This trend suggests that paclitaxel has been taken up by the cells. The data for cells incubated with only DMSO was not shown since it is not statistically different from the results of the untreated cell culture indicating the two control groups were comparable and DMSO had no effect on paclitaxel transport. It was hypothesized that the inhibitors would inhibit the uptake of the paclitaxel so more paclitaxel would remain in the media. Also, higher inhibitor concentrations may have a more significant effect. However, other than the general trend showing paclitaxel uptake, concrete conclusions about paclitaxel transport mechanism cannot be made when taking the results of statistical analysis into consideration. In the media samples, the difference in concentrations of paclitaxel in each treatment group and control group was not statistically significant. This suggests that a 0.17 μM inhibitor solution does not affect the transport mechanism of paclitaxel within the system of study. When the cells were treated with higher concentrations of verapamil, cyclosporine A and genistein, the concentration of paclitaxel in the media is significantly lower than that of the control group after 6 hours. This result indicates a potential facilitation of uptake by the inhibitors. However, this potential facilitation is transient since the concentrations of paclitaxel in the inhibitor treated

groups were comparable with that in the control group after 24 hours incubation. The same result was observed, but earlier in the experiment, for the vanadate treated group. When a higher concentration of vanadate is added, the concentration of paclitaxel in the media is significant lower than the control group after 1.5 hours. However, paclitaxel concentrations are comparable with that of control group during the rest of the experiment. Therefore, the significant effects of inhibitors were transient and there was no consistent trend.

According to the cell-associated samples, the inhibitors generally had an effect at lower concentrations. The paclitaxel concentration in verapamil and cyclosporine A treated groups was significantly lower than the control group after incubation for 6 hours, indicating potential inhibition of uptake. However, the paclitaxel concentration in the vanadate treated group was significantly higher than the control group, which could be a potential facilitation of uptake. Similar with the results seen for the media samples, the phenomena demonstrated in the cell-associated samples was also transient and could not be observed at the next time point.

Observations based on the cell-associated samples did not agree with observations based on media samples. This could be explained by errors in the experiment design. First, the amount of paclitaxel in the cell-associated samples are not normalized to the sample volumes, and a volume of 1 mL was assumed for each sample. During the experiment, 1 mL of cell samples were taken and processed for paclitaxel concentration analyses. However, since the sample was taken directly from the suspension culture, there was media in the cell samples, which was removed before sample processing. In other words, the actual volume of the cell samples was less than 1 mL, varies across the samples, and final cell volumes are unknown. Although triplicate biological samples had been run to reduce the effect of the variation in the final data, the cell volume could certainly affect the statistical analysis and make it hard to decipher a trend from the results.

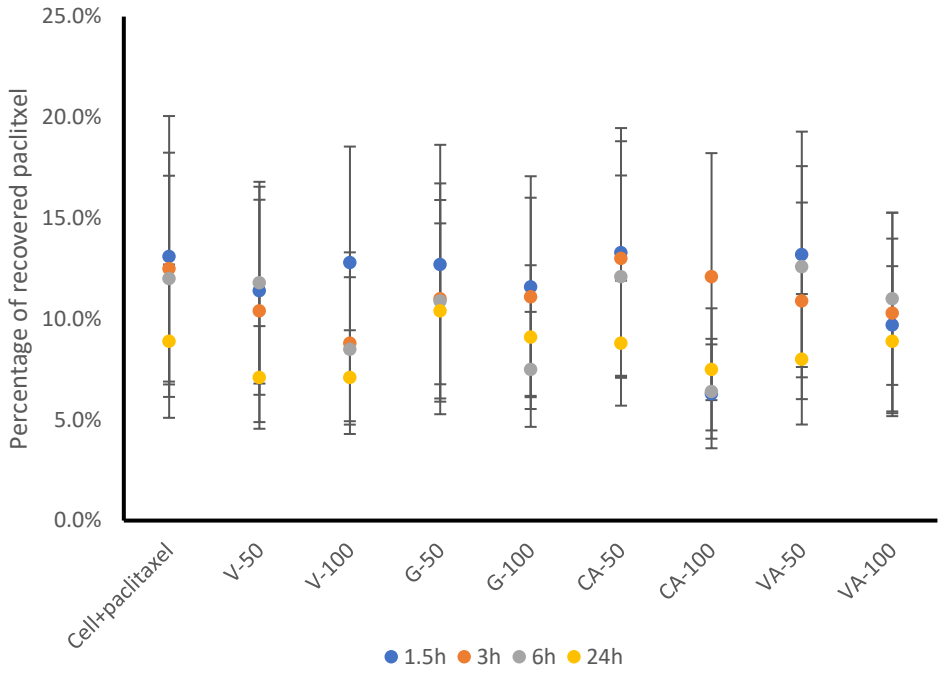

Figure 18. Percent recovery of paclitaxel in the preliminary inhibitor test. The recovery percentages were obtained by calculating the total mass of paclitaxel recovered in media and cell samples and compared with the total mass of paclitaxel added into the culture at the beginning of the experiment.

The highest percentage of paclitaxel recovery is 13.3 ± 6.2% among all the samples (Figure 18). In other words, the majority of the paclitaxel was lost during the experiment and/or sample processing. There are two main reasons likely for the low recovery. One is the incorrect processing procedure for the media samples. During the sample processing, the media samples from cell culture were centrifuged and only the supernatant was obtained for the next process step. However, since paclitaxel is a hydrophobic molecule, it associates with suspended proteins, tissues or other cellular debris in the media. Once the media sample was centrifuged, the higher concentration of paclitaxel would more likely be in the pellet instead of the supernatant. Therefore, significant paclitaxel may have been lost at the beginning of the sample processing. Another possibility is overestimation of cell volume. Since the actual volume of each sample was unknown, the recovery was calculated based on 1 mL of cell sample. However, as mentioned previously, the actual volume of the cells was less than 1 mL in each sample once the media was removed. This overestimation of cell volume causes an underestimation of the paclitaxel recovery. Since the amount of unaccounted paclitaxel cannot be accurately determined for media or cell samples, variations were created and results could be affected.

4.2.3 Investigation of the effect of concentration on inhibition

Among all the results given through the initial inhibitor test, the verapamil treated cells show the clearest trends in influencing paclitaxel transport. To further investigate inhibition of the paclitaxel transport mechanism, verapamil was evaluated at a higher concentration and samples were taken at more time points (Figure 19),

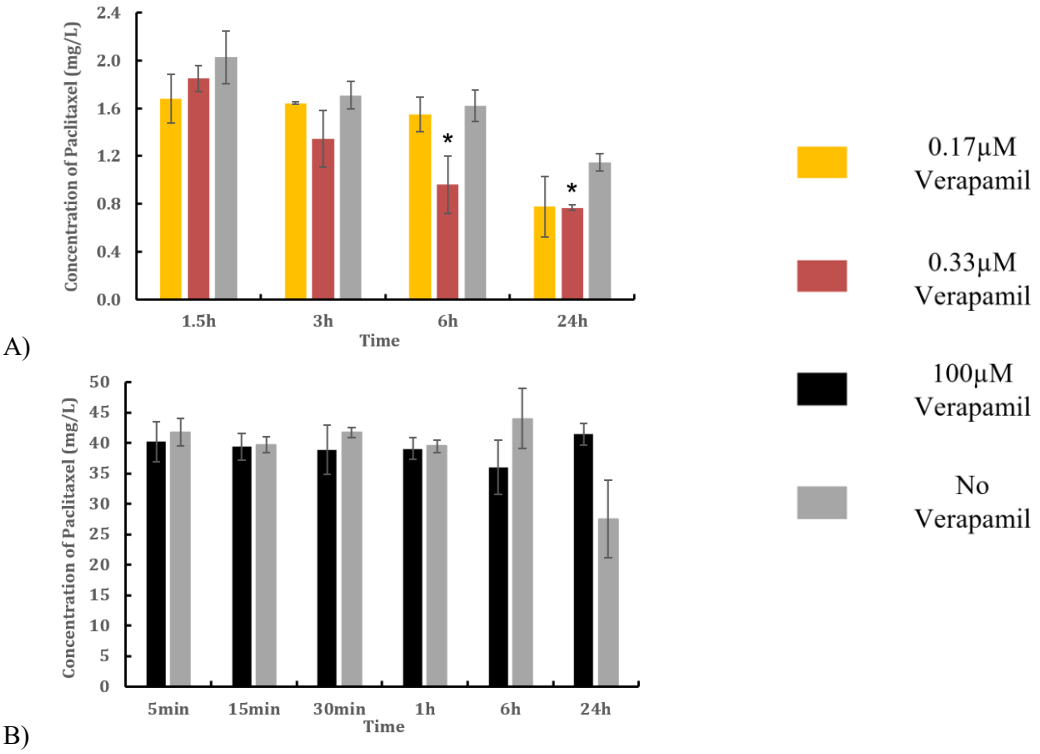

Figure 19. A) Subset media sample data from the previous experiment with verapamil treatment, B) Paclitaxel concentration in media with increased concentration of verapamil *=$p<0.05$ as compare to control according to Student's t-test, N=3. The error bars represent the standard deviation of triplicates.

According to Figure 19A, when the final concentration of verapamil in the cell culture is 0.17 μM or 0.33 μM, the concentration of paclitaxel in the media was lower than that in the control group after 24 hours. This indicates the verapamil treatment is facilitating the uptake of paclitaxel. However, when the final concentration of verapamil was 100 μM in the cell culture the concentration of paclitaxel in the media was higher than that in the control group (Figure 19B), indicating an inhibition of paclitaxel uptake by verapamil. Moreover, the facilitation of the uptake for 0.33 μM started after incubation for 6 hours, while the inhibition of 100 μM verapamil occurred after 24 hours of incubation. More tests are certainly needed to make concrete conclusions about

the correlation of the verapamil concentration and paclitaxel transport direction and the action time of the verapamil inhibition. However, these experiments indicate that that verapamil has an effect on paclitaxel transport, suggesting that a MDR-type protein may be involved.

4.3Alternative paclitaxel quantification technique

4.3.1 Establishing a paclitaxel concentration calibration curve with UV-vis technologies

To investigate the potential of using UV-vis spectroscopy for paclitaxel concentration, media and cell samples that had been tested in UPLC were tested in UV-vis spectroscopy. The UV-vis spectra are shown in Figure 20.

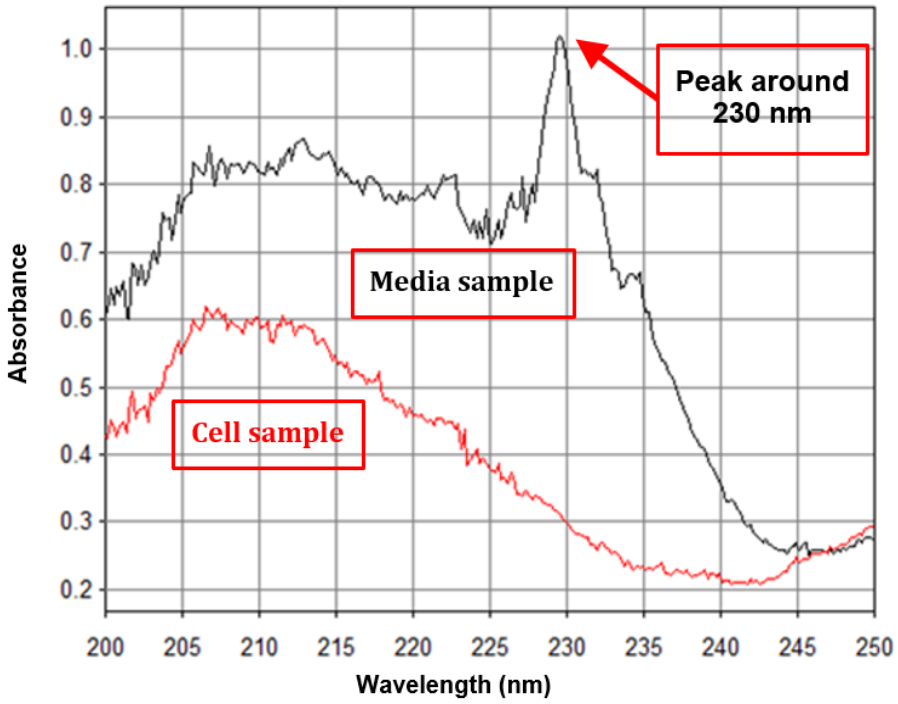

Figure 20. UV-vis spectra of UPLC media and cell samples. The red line represents the spectrum of cell sample and the black line represents the spectrum of media sample.

As shown in Figure 20, a peak at 230 nm wavelength with absorbance around 1, is detected in the media sample. Since the peak at 230 nm is used to characterize paclitaxel, it is likely that the peak on the media UV-vis spectrum at that wavelength represents the paclitaxel in the media sample. This led us to believe that UV-vis could be an alternative method for paclitaxel quantification. It was also noticed that on the spectrum of the cell sample, there was no peak at 230 nm (Figure 20).

The lack of peak could be a result of several reasons including undetectable paclitaxel levels or the interference of absorption of paclitaxel by other cellular components.

To further investigate development of a protocol to quantify paclitaxel with UV-vis, a calibration curve of absorbance against paclitaxel concentration was generated. (Figure 21).

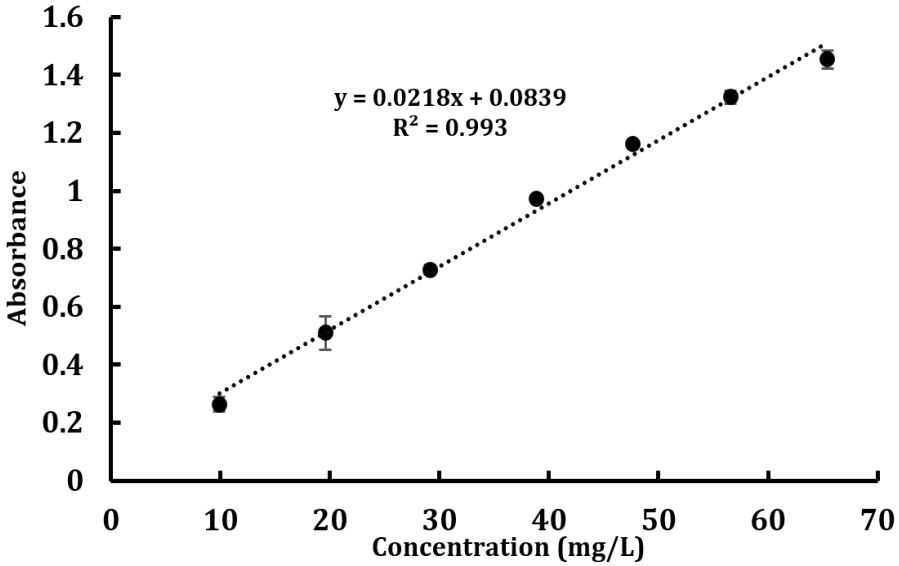

Figure 21. Standard calibration curve of paclitaxel in water-acetonitrile solution

According to Figure 21. there is a strong linear correlation of the absorbance and the paclitaxel concentrations within the range of 10 mg/L to 65 mg/L. The upper limit that can be tested is 70 mg/L since paclitaxel is not soluble in water-acetonitrile solution at higher concentrations. The lower limit was 10 mg/L because the paclitaxel peak is not distinguishable when concentrations below were tested. Overall, the linear calibration curve indicates that any concentration of paclitaxel in water-acetonitrile solution can be easily and accurately quantified within the range of 10 to 65 mg/L using the UV-vis.

After seeing the promising correlation of the absorbance and paclitaxel concentration in pure water-acetonitrile solutions, the absorbance of paclitaxel was also tested in *Taxus* media-based samples. As mentioned in the methodology, the media-based samples were processed using the same protocol for typical UPLC analyzed samples with different concentrations of paclitaxel in fresh media. The results are shown in Figure 22.

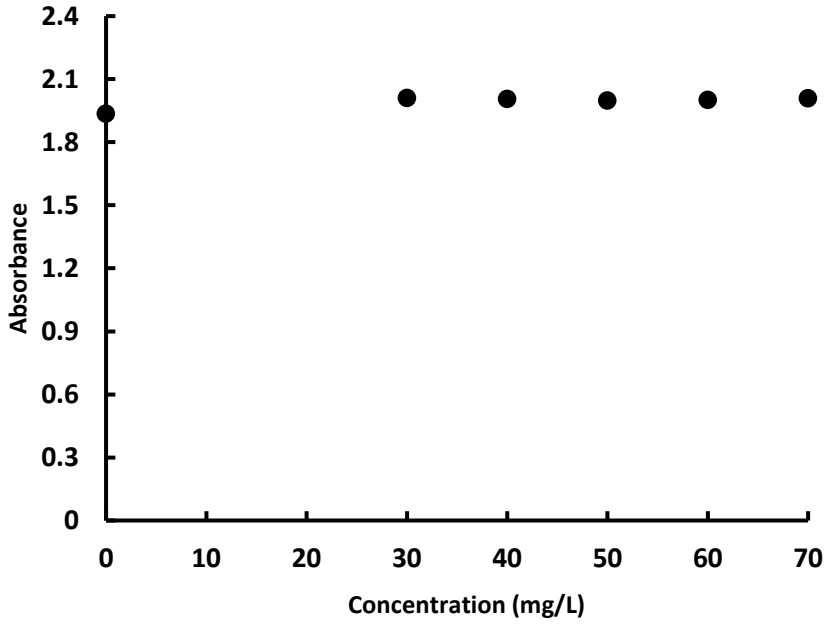

Figure 22. Absorbance of different concentrations of paclitaxel in media based solution in UV-vis spectroscopy

As shown in Figure 22, the absorbance of media is independent of the paclitaxel concentration. Regardless of the concentration, the absorbance at 230 nm wavelength was around 2. The strong absorbance in the spectra of media-based samples indicates that there are interfering component(s) in the fresh media that have the same absorbance as paclitaxel.

4.3.2 Identification of the interfering compound(s)

There are four main components in the media: Gamborg B5, sucrose, 6-benzylaminopurine (BA), and naphthaleneacetic acid (NAA). Four of them were dissolved separately in the nanopore water at their appropriate media concentration and their UV-vis spectra were obtained (Figure 23).

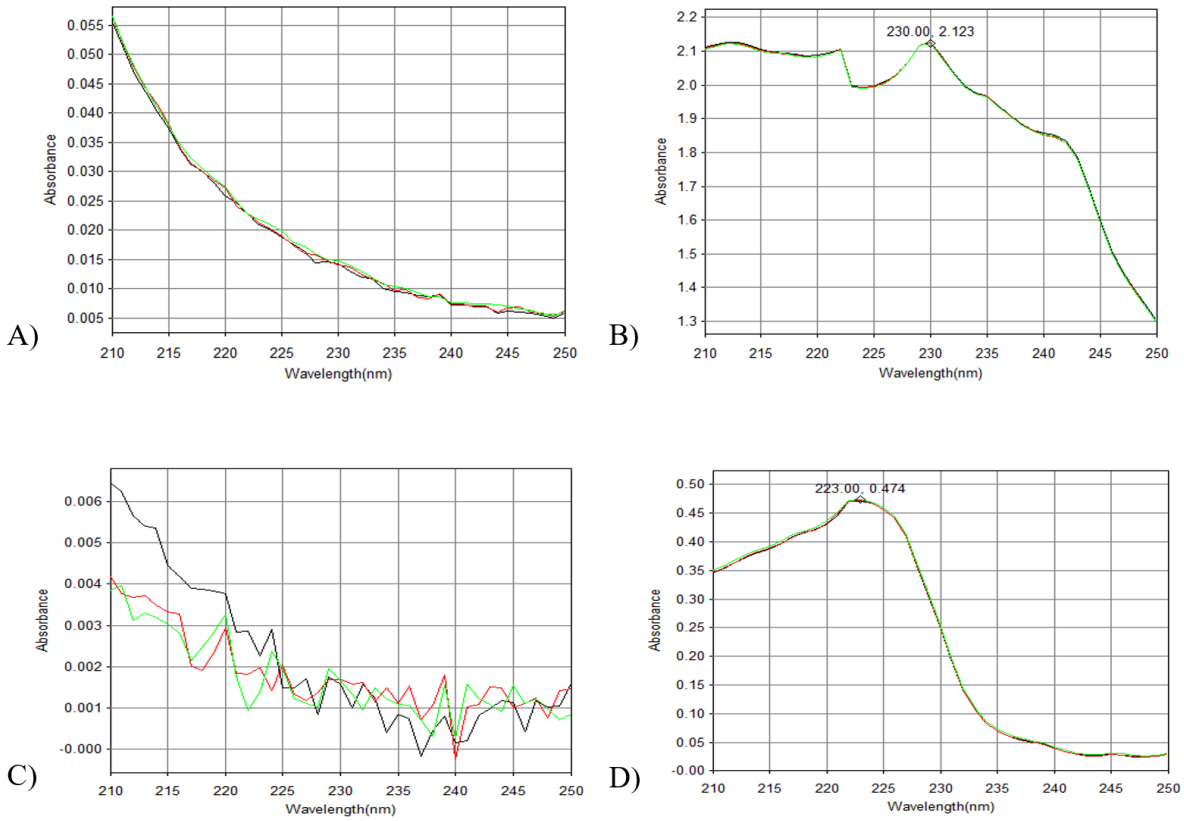

Figure 23. UV-vis spectrum of A) sucrose B) Gamborg B5 salts C) BA D) NAA. Green, red, and black represent three different trials

Gamborg B5 is the only media component that has a strong absorbance of 2.1 at 230 nm. The spectra of nanopure water and acetonitrile was also obtained, but no peak showed up at 230 nm. Since Gamborg B5 is the only component showing a peak at 230 nm, and its absorbance is comparable with the results in the media-based sample tests, it is most likely the interfering component in the UV-vis test. Since it can be detected in both water-based samples and water-acetonitrile-based sample after UPLC sample processing, Gamborg B5 must be soluble in all of the solvents used for extraction. Specifically, it is soluble in water, methanol and water-acetonitrile solutions. In fact, Gamborg B5 is a mixture of vitamins and minerals commonly used in the plant cell culture (59). As the interfering component in the test, Gamborg B5 is an essential element of the plant cell culture media and cannot be eliminated from the experimental setup. Therefore UV-vis spectroscopy cannot be used as an alternative method for quantifying paclitaxel.

5. Conclusion

Based on the experimental results, there are three major conclusions that can be made. First, in the bioinformatics analysis, the high percentage identity and similarity with mammalian MDR proteins, especially at the function domains suggested that E6Y0T0 is a potential transport protein of paclitaxel in *Taxus* cells. Second, in the inhibitor tests, it was shown that verapamil affects paclitaxel transport, supporting an MDR-like transport mechanism. Third, the investigation of an alternative paclitaxel quantification technique has shown that UV-vis spectroscopy cannot be used to test paclitaxel concentration with the current *Taxus* experimental setup.

6. Future directions

Future experiments should include isolating E6Y0T) and expressing it in *Saccharomyces cerevisiae* to determine its function and biochemical activity. If found indeed to be the paclitaxel transport protein, a genetically modified cell line overexpressing the transport protein could be developed to increase secretion to the media and improve recovery and purification of paclitaxel. Inhibitor tests should be repeated and expanded including optimizing concentrations and redesigning experimental protocols to enable a mass balance on the paclitaxel added to the cultures. All of these recommendations for future experiments should be implemented in order to fully characterize paclitaxel transport to optimize the downstream process of paclitaxel bioprocessing.

7. References

(1) Miller, H. I. (2001). The Story of Taxol: Nature and Politics in the Pursuit of an Anti-Cancer Drug. *Nature Medicine*, *7*(2), 148. Retrieved from http://libraries.state.ma.us/login?gwurl=http://link.galegroup.com/apps/doc/A193842758/SCIC?u=mlin_c_worpoly&xid=3ce0214f

(2) Schiff PB, Fant J, Horwitz SB. Promotion of microtubule assembly in vitro by Taxol. Nature. 1979;277:665–667.

(3) Weaver, B. A. (2014). How Taxol/paclitaxel kills cancer cells. *Molecular Biology of the Cell*, *25*(18), 2677–2681. http://doi.org/10.1091/mbc.E14-04-0916

(4) Bharadwaj R., Yu H. (2004). "The spindle checkpoint, aneuploidy, and cancer". Oncogene 23 (11): 2016–27. doi:10.1038/sj.onc.1207374. PMID 15021889.

(5) Jordan MA, Leslie W, Microtubules as a target for anticancer drugs Apr 4, 2004",

(6) Brito D. A., Yang Z., Rieder C. L. (2008). "Microtubules do not promote mitotic slippage when the spindle assembly checkpoint cannot be satisfied". J. Cell Biol. 182 (4): 623–9. doi:10.1083/jcb.200805072. PMC 2518701. PMID 18710927.

(7) How Does Taxol WorkRetrieved April 23, 2017, from http://www.medicalnewstoday.com/opinions/176471

(8)UK, C. R. (n.d.). Paclitaxel (Taxol). Retrieved April 23, 2017, from http://www.cancerresearchuk.org/about-cancer/cancers-in-general/treatment/cancer-drugs/paclitaxel
(9)Paclitaxel. (n.d.). Retrieved April 23, 2017, from https://pubchem.ncbi.nlm.nih.gov/compound/paclitaxel#section=Top

(10) Paclitaxel. (n.d.). Retrieved April 24, 2017, from https://www.drugbank.ca/drugs/DB01229

(11) Paclitaxel (n.d.). Retrieved April 23, 2017, from http://www4.mpbio.com/ecom/docs/proddata.nsf/(webtds2)/193532

(12) Ambudkar, S. V., Kimchi-Sarfaty, C., Sauna, Z. E., & Gottesman, M. M. (2003). P-glycoprotein: from genomics to mechanism. *Oncogene*, *22*(47), 7468-7485.

(13) Paclitaxel. Retrieved April 24, 2017, from http://www.newdruginfo.com/pharmacopeia/usp28/v28230/usp28nf23s0_m60190.htm

(14) Wani MC, Taylor HL, Wall ME, Coggon P, McPhail AT. Plant antitumor agents. VI. The isolation and structure of taxol, a novel antileukemic and antitumor agent from Taxus brevifolia. J Am Chem Soc. 1971;93:2325–2327.

(15) Kawamura, F., Kikuchi, Y., Ohira, T., & Yatagai, M. (1999). Accelerated solvent extraction of paclitaxel and related compounds from the bark of Taxus cuspidata. *Journal of natural products*, *62*(2), 244-247.

(16) Solvent extraction in English. (n.d.). Retrieved April 23, 2017, from https://glosbe.com/en/en/solvent%20extraction

(17) The Editors of Encyclopædia Britannica. (2008, September 03). Pacific yew. Retrieved April 23, 2017, from http://www.britannica.com/plant/Pacific-yew

(18) Nicolaou, K. C., Guy, R. K., & Potier, P. (1996). Taxoids: new weapons against cancer. *Scientific American*, *274*(6), 84-8.

(19)Taxus Brevifolia Nutt. Retrieved April 23, 2017, from http://www.na.fs.fed.us/spfo/pubs/silvics_manual/Volume_1/taxus/brevifolia.htm

(20) Guerra-Bubb, J., Croteau, R., & Williams, R. M. (2012). The Early Stages of Taxol Biosynthesis: An Interim Report on the Synthesis and Identification of Early Pathway Metabolites. *Natural Product Reports*, *29*(6), 683–696. http://doi.org/10.1039/c2np20021j

(21) K. C. Nicolaou, Z. Zang, J. J. Liu, H. Ueno, P. G. Nantermet, R. K. Guy, C. F. Claiborne, J. Renaud, E. A. Couladouros, K. Paulvannan and E. J. Sorensen, *Nature*, 1994, 367, 630 ; K. C. Nicolaou, P. G. Nantermet, H. Ueno, R. K. Guy, E. A. Couladouros and E. J. Sorenson, *J. Am. Chem. Soc.*, 1995, 117, 624; K. C. Nicolaou, J. J. Liu, Z. Yang, H. Ueno, E. J. Sorenson, C. F. Claiborne, R. K. Guy, C. K. Hwang, M. Nakada and P. G. Nantermet, *J. Am. Chem. Soc.*, 1995, 117, 634;K. C. Nicolaou, Z. Yang, J. J. Liu, P. G. Nantermet, C. F. Claiborne, J. Renaud, R. K. Guy and K. Shibayama, *J. Am. Chem. Soc.*, 1995, 117, 645.

(22) R. A. Holton, C. Somoza, H. B. Kim, F. Liang, R. J. Biediger, P. D. Boatman, M. Shindo, C. C. Smith, S. C. Kim, H. Nadizadeh, Y. Suzuki, C. L. Tao, P. Vu, S. H. Tang, P. S. Zhang, K. K. Murthi, L. N. Gentile and J. H. Liu, *J. Am. Chem. Soc.*, 1994, 116, 1597 ; R. A. Holton, H. B. Kim, C. Somoza, F. Liang, R. J. Biediger, P. D. Boatman, M. Shindo, C. C. Smith, S. C. Kim, H. Nadizadeh, Y. Suzuki, C. L. Tao, P. Vu, S. H. Tang, P. S. Zhang, K. K. Murthi, L. N. Gentile and J. H. Liu, *J. Am. Chem. Soc.*, 1994, 116, 1599

(23) Nicolaou Taxol total synthesis. (2016, November 11). Retrieved April 23, 2017, from https://en.wikipedia.org/wiki/Nicolaou_Taxol_total_synthesis

(24) Rao, K. V. (1997). Semi-synthesis of paclitaxel from naturally occurring glycosidic precursors. *Journal of heterocyclic chemistry*, *34*(2), 675-680

(25) Share and discover research. (n.d.). Retrieved April 23, 2017, from http://www.researchgate.net/figure/262809023_fig1_Figure-1-Structures-of-taxol-the-semisynthetic-derivative-taxotere-and-the-two

(26) PhD, D. T. (2014, October 21). Paclitaxel Production. Retrieved April 23, 2017, from http://www.news-medical.net/health/Paclitaxel-Production.aspx

(27) Bristol-Myers Squibb. (n.d.). Retrieved April 23, 2017, from http://pcm.me/bristol-myers-squibb/

(28) Hellwig, S., Drossard, J., Twyman, R. M., & Fischer, R. (2004, November 04). Plant cell cultures for the production of recombinant proteins. Retrieved April 23, 2017, from http://www.nature.com/nbt/journal/v22/n11/full/nbt1027.html

(29) Roberts, S.C., Naill, M., Gibson, D.M. et al. Plant Cell Rep (2003) 21: 1217. doi:10.1007/s00299-003-0575-z

(30) McPartland, T. J., Patil, R. A., Malone, M. F., & Roberts, S. C. (2012). Liquid-Liquid Extraction for Recovery of Paclitaxel from Plant Cell Culture: Solvent Evaluation and Use of Extractants for Partitioning and Selectivity. *Biotechnology Progress*, *28*(4), 990–997. http://doi.org/10.1002/btpr.1562

(31) Vasiliou V, Vasiliou K, Nebert DW. Human ATP-binding cassette (ABC) transporter family. *Human Genomics*. 2009;3(3):281-290. doi:10.1186/1479-7364-3-3-281.

(32) Gottesman, M. M. (2002). Mechanisms of cancer drug resistance. *Annual review of medicine*, *53*(1), 615-627.

(33) Choudhuri, S., & Klaassen, C. D. (2006). Structure, function, expression, genomic organization, and single nucleotide polymorphisms of human ABCB1 (MDR1), ABCC (MRP), and ABCG2 (BCRP) efflux transporters. *International journal of toxicology*, *25*(4), 231-259

(34) Aller, S. G., Yu, J., Ward, A., Weng, Y., Chittaboina, S., Zhuo, R., ... & Chang, G. (2009). Structure of P-glycoprotein reveals a molecular basis for poly-specific drug binding. *Science*, *323*(5922), 1718-1722.

(35) Yazaki, Kazufumi. "ABC Transporters Involved in the Transport of Plant Secondary Metabolites." *FEBS Letters* 580.4 (2006): 1183-191. Web. 2 Apr. 2017.

(36) Yazaki, K., Shitan, N., Takamatsu, H., Ueda, K., & Sato, F. (2001). A novel Coptis japonica multidrug-resistant protein preferentially expressed in the alkaloid-accumulating rhizome. *Journal of experimental botany*, *52*(357), 877-879.

(37) Shitan, N., Bazin, I., Dan, K., Obata, K., Kigawa, K., Ueda, K., ... & Yazaki, K. (2003). Involvement of CjMDR1, a plant multidrug-resistance-type ATP-binding cassette protein, in alkaloid transport in Coptis japonica. *Proceedings of the National Academy of Sciences*, *100*(2), 751-756.

(38) Ravna, A. W., Sylte, I., & Sager, G. (2007). Molecular model of the outward facing state of the human P-glycoprotein (ABCB1), and comparison to a model of the human MRP5 (ABCC5). *Theoretical Biology and Medical Modelling*, 4(1), 33.

(39) Fornalè, S., Degli Esposti, D., Navia-Osorio, A., Cusidò, R. M., Palazòn, J., Piñol, M. T., & Bagni, N. (2002). Taxol transport in Taxus baccata cell suspension cultures. *Plant Physiology and Biochemistry*, *40*(1), 81-88.

(40) Naill, M. C., Kolewe, M. E., & Roberts, S. C. (2012). Paclitaxel uptake and transport in Taxus cell suspension cultures. *Biochemical engineering journal*, *63*, 50-56.

(41) Duan, Z., Brakora, K. A., & Seiden, M. V. (2004). Inhibition of ABCB1 (MDR1) and ABCB4 (MDR3) expression by small interfering RNA and reversal of paclitaxel resistance in human ovarian cancer cells. *Molecular cancer therapeutics*, *3*(7), 833-838.

(42) Fassler J, Cooper P. BLAST Glossary. 2011 Jul 14. In: BLAST® Help [Internet]. Bethesda (MD): National Center for Biotechnology Information (US); 2008-. Available from: https://www.ncbi.nlm.nih.gov/books/NBK62051/

(43) Pearson, W. R. (2013). An introduction to sequence similarity ("homology") searching. *Current protocols in bioinformatics*, 3-1.

(44) PCR Primer Design Guidelines. (n.d.). Retrieved April 23, 2017, from http://www.premierbiosoft.com/tech_notes/PCR_Primer_Design.html

(45) Biolabs, N. E. (n.d.). Polymerase Fidelity: What is it, and what does it mean for your PCR? Retrieved April 24, 2017, from https://www.neb.com/tools-and-resources/feature-articles/polymerase-fidelity-what-is-it-and-what-does-it-mean-for-your-pcr

(46) Biolabs, N. E. (n.d.). Q5® High-Fidelity DNA Polymerases. Retrieved April 24, 2017, from https://www.neb.com/products/pcr-polymerases-and-amplification-technologies/q5-high-fidelity-dna-polymerases/q5-high-fidelity-dna-polymerases

(47) Callaghan, R., Luk, F., & Bebawy, M. (2014). Inhibition of the multidrug resistance P-glycoprotein: time for a change of strategy?. *Drug Metabolism and Disposition*, *42*(4), 623-631.

(48) Sakai, K., Shitan, N., Sato, F., Ueda, K., & Yazaki, K. (2002). Characterization of berberine transport into Coptis japonica cells and the involvement of ABC protein. *Journal of experimental botany*, *53*(376), 1879-1886.
(49) Amin, M. L. (2013). P-glycoprotein inhibition for optimal drug delivery. *Drug target insights*, *7*, 27.

(50) Perez, M., Otero, J. A., Barrera, B., Prieto, J. G., Merino, G., & Alvarez, A. I. (2013). Inhibition of ABCG2/BCRP transporter by soy isoflavones genistein and daidzein: effect on plasma and milk levels of danofloxacin in sheep. *The Veterinary Journal*, *196*(2), 203-208.

(51) Kim, H., Peterson, T. G., & Barnes, S. (1998). Mechanisms of action of the soy isoflavone genistein: emerging role for its effects via transforming growth factor beta signaling pathways. *The American journal of clinical nutrition*, *68*(6), 1418S-1425S.

(52) Boyd, V., Cholewa, O. M., & Papas, K. K. (2008). Limitations in the use of fluorescein diacetate/propidium iodide (FDA/PI) and cell permeable nucleic acid stains for viability measurements of isolated islets of Langerhans. *Current trends in biotechnology and pharmacy*, *2*(2), 66.

(53) Swartz, M. E. (2005). UPLC™: an introduction and review. *Journal of Liquid Chromatography & Related Technologies*, *28*(7-8), 1253-1263.

(54) Skoog, D. A., Holler, F. J., & Crouch, S. R. (2007). *Principles of instrumental analysis*. Thomson Brooks/Cole. pp. 169–173

(55) Dhole, S. M., Amnerkar, N. D., & Khedekar, P. B. (2012). Comparison of UV spectrophotometry and high performance liquid chromatography methods for the determination of repaglinide in tablets. *Pharmaceutical Methods*, *3*(2), 68-72.

(56) Vieira, D. C. M., & Salgado, H. R. N. (2011). Comparison of HPLC and UV spectrophotometric methods for the determination of cefuroxime sodium in pharmaceutical products. *Journal of chromatographic science*, *49*(7), 508-511.

(57) Kesarwani, P., Tekade, R. K., & Jain, N. K. (2011). Spectrophotometric estimation of paclitaxel. *International Journal of Advances in Pharmaceutical Sciences*, *2*(1).
(58) Cheng, S., Fockler, C., Barnes, W. M., & Higuchi, R. (1994). Effective amplification of long targets from cloned inserts and human genomic DNA. *Proceedings of the National Academy of Sciences*, *91*(12), 5695-5699.

(59) Gamborg, O. L., Miller, R., & Ojima, K. (1968). Nutrient requirements of suspension cultures of soybean root cells. *Experimental cell research*, *50*(1), 151-158.

8. Appendix

Appendix A: Protein Sequences

Sequence of E6Y0T0

>tr|E6Y0T0|E6Y0T0_TAXCU MDR-like ABC transporter OS=Taxus cuspidata GN=mdr PE=2 SV=1

MPKEGDNSNDGNHDHGAVSLNIEKVSEMNSNMAKAKDKKKKENNKVVPFHKLFVTADSLD
KLLMALGTIGAVANGVSIPLMTILFGGLINAFGENSTDGKKVMNEVSKLALEFVYLACGA
GVASLLQVSCWMCTGERQATRIRSLYLKTILRQDIGFFDSEASTGEVIGRMSGDTILIQD
AMGEKVGKFIQFITTFIAGFVIAFIKGWKLSLVMLSMIPLLVVSGGSMAMIISKMSSRGQ
QAYSEAANIVEQTIGSIRMVASFTGEKKSIEGYNKSLAIAYNAITQQGLVAGVGLGSVLF
IMFCGYALALWYGSRLILDGSYTGGDVINVIFAVLMGGMSLGQTSPSLNAFSAGRAAAYK
MFETIDRKPVIDVFDKSGLVLEDIQGDIELKDVRFTYPARPDVQVFSGFSLEIPSGTTAA
LVGESGSGKSTVISLVERFYDPQAGEVLIDGINIKKFQLKWIRQKIGLVSQEPVLFGTTI
KENLLYGKDGATLEEIKAAAELANAAKFINKLPQGFDTMVGEHGTQLSGGQKQRIAIARA
ILKDPRILLLDEATSALDTESERVVQEALDRIMVNRTTVIVAHRLTTVRNADMIAVVQRG
SIVEKGSHSQLITNPSGAYSQLIHLQESNRSKEQDSKDPDELEIHQDDSKVLGRVSSQRS
SFRRSISSGSSGIGGSRRSYSFSYAFPGTVGLQETGGMEEISQSKGNKRRKGLMSYFRSN
TQKDVEGGQSDAEKDVSILRLASLNKPEIPVFILGSIAAAMNGMIFPVFGLLLSSVIKVF
YEPPHELRKDAKFWALMFIVLAVTCFIVAPTQMYCFSIAGGRLVQRIRSLTFSKVVYQEI
SWFDDNENSSGAISARLSTDAATVRSLVGDALSLVVQNIATIIAGIVISFTANWLLALLI
LAIVPLLGLQGYMQVKFMTGFTADAKLVYEEASQVANDAVGSIRTVASFCAEDKVISLYN
EKCSAPLKSGVKQGIIAGLGLGFSNFVMFTQYALSFWVGARLVEDGKTTFDKVFKVFFAL
SMAAAGISQSAGLSPDLAKAKSSINSVFKILDRPSKIDANDESGTILDNVKGDIEFQHVS
FKYPTRPDVQIFRDLCLFVHSGKTVALVGESGSGKSTAIALLERFYDPDSGRIFLDGVEI
RQLQLKWLRQQMGLVSQEPVLFNDTIRANIAYGKEGAVTDEQIIAAAEAANAHKFISSLP
QGYNINVGERGVQLSGGQKQRIAIARAILKDPRILLLDEATSALDAESERIVQDALDRVK
VNRSTIVIAHRLSTIKDADLIAVVKNGKIAEQGKHDELLKKRNGAYASLVQLHKSS

Sequence of ABCB1

>sp|P08183|MDR1_HUMAN Multidrug resistance protein 1 OS=Homo sapiens GN=ABCB1 PE=1 SV=3

MDLEGDRNGGAKKKNFFKLNNKSEKDKKEKKPTVSVFSMFRYSNWLDKLYMVVGTLAAII
HGAGLPLMMLVFGEMTDIFANAGNLEDLMSNITNRSDINDTGFFMNLEEDMTRYAYYYSG
IGAGVLVAAYIQVSFWCLAAGRQIHKIRKQFFHAIMRQEIGWFDVHDVGELNTRLTDDVS
KINEGIGDKIGMFFQSMATFFTGFIVGFTRGWKLTLVILAISPVLGLSAAVWAKILSSFT
DKELLAYAKAGAVAEEVLAAIRTVIAFGGQKKELERYNKNLEEAKRIGIKKAITANISIG
AAFLLIYASYALAFWYGTTLVLSGEYSIGQVLTVFFSVLIGAFSVGQASPSIEAFANARG
AAYEIFKIIDNKPSIDSYSKSGHKPDNIKGNLEFRNVHFSYPSRKEVKILKGLNLKVQSG
QTVALVGNSGCGKSTTVQLMQRLYDPTEGMVSVDGQDIRTINVRFLREIIGVVSQEPVLF
ATTIAENIRYGRENVTMDEIEKAVKEANAYDFIMKLPHKFDTLVGERGAQLSGGQKQRIA
IARALVRNPKILLLDEATSALDTESEAVVQVALDKARKGRTTIVIAHRLSTVRNADVIAG
FDDGVIVEKGNHDELMKEKGIYFKLVTMQTAGNEVELENAADESKSEIDALEMSSNDSRS
SLIRKRSTRRSVRGSQAQDRKLSTKEALDESIPPVSFWRIMKLNLTEWPYFVVGVFCAII
NGGLQPAFAIIFSKIIGVFTRIDDPETKRQNSNLFSLLFLALGIISFITFFLQGFTFGKA
GEILTKRLRYMVFRSMLRQDVSWFDDPKNTTGALTTRLANDAAQVKGAIGSRLAVITQNI
ANLGTGIIISFIYGWQLTLLLLAIVPIIAIAGVVEMKMLSGQALKDKKELEGSGKIATEA
IENFRTVVSLTQEQKFEHMYAQSLQVPYRNSLRKAHIFGITFSFTQAMMYFSYAGCFRFG
AYLVAHKLMSFEDVLLVFSAVVFGAMAVGQVSSFAPDYAKAKISAAHIIMIIEKTPLIDS
YSTEGLMPNTLEGNVTFGEVVFNYPTRPDIPVLQGLSLEVKKGQTLALVGSSGCGKSTVV
QLLERFYDPLAGKVLLDGKEIKRLNVQWLRAHLGIVSQEPILFDCSIAENIAYGDNSRVV
SQEEIVRAAKEANIHAFIESLPNKYSTKVGDKGTQLSGGQKQRIAIARALVRQPHILLLD
EATSALDTESEKVVQEALDKAREGRTCIVIAHRLSTIQNADLIVVFQNGRVKEHGTHQQL

LAQKGIYFSMVSVQAGTKRQ

Sequence of ABCB4

>sp|P21439|MDR3_HUMAN Phosphatidylcholine translocator ABCB4 OS=Homo sapiens GN=ABCB4 PE=1 SV=2
MDLEAAKNGTAWRPTSAEGDFELGISSKQKRKKTKTVKMIGVLTLFRYSDWQDKLFMSLG
TIMAIAHGSGLPLMMIVFGEMTDKFVDTAGNFSFPVNFSLSLLNPGKILEEEMTRYAYYY
SGLGAGVLVAAYIQVSFWTLAAGRQIRKIRQKFFHAILRQEIGWFDINDTTELNTRLTDD
ISKISEGIGDKVGMFFQAVATFFAGFIVGFIRGWKLTLVIMAISPILGLSAAVWAKILSA
FSDKELAAYAKAGAVAEEALGAIRTVIAFGGQNKELERYQKHLENAKEIGIKKAISANIS
MGIAFLLIYASYALAFWYGSTLVISKEYTIGNAMTVFFSILIGAFSVGQAAPCIDAFANA
RGAAYVIFDIIDNNPKIDSFSERGHKPDSIKGNLEFNDVHFSYPSRANVKILKGLNLKVQ
SGQTVALVGSSGCGKSTTVQLIQRLYDPDEGTINIDGQDIRNFNVNYLREIIGVVSQEPV
LFSTTIAENICYGRGNVTMDEIKKAVKEANAYEFIMKLPQKFDTLVGERGAQLSGGQKQR
IAIARALVRNPKILLLDEATSALDTESEAEVQAALDKAREGRTTIVIAHRLSTVRNADVI
AGFEDGVIVEQGSHSELMKKEGVYFKLVNMQTSGSQIQSEEFELNDEKAATRMAPNGWKS
RLFRHSTQKNLKNSQMCQKSLDVETDGLEANVPPVSFLKVLKLNKTEWPYFVVGTVCAIA
NGGLQPAFSVIFSEIIAIFGPGDDAVKQQKCNIFSLIFLFLGIISFFTFFLQGFTFGKAG
EILTRRLRSMAFKAMLRQDMSWFDDHKNSTGALSTRLATDAAQVQGATGTRLALIAQNIA
NLGTGIIISFIYGWQLTLLLLAVVPIIAVSGIVEMKLLAGNAKRDKKELEAAGKIATEAI
ENIRTVVSLTQERKFESMYVEKLYGPYRNSVQKAHIYGITFSISQAFMYFSYAGCFRFGA
YLIVNGHMRFRDVILVFSAIVFGAVALGHASSFAPDYAKAKLSAAHLFMLFERQPLIDSY
SEEGLKPDKFEGNITFNEVVFNYPTRANVPVLQGLSLEVKKGQTLALVGSSGCGKSTVVQ
LLERFYDPLAGTVFVDFGFQLLDGQEAKKLNVQWLRAQLGIVSQEPILFDCSIAENIAYG
DNSRVVSQDEIVSAAKAANIHPFIETLPHKYETRVGDKGTQLSGGQKQRIAIARALIRQP
QILLLDEATSALDTESEKVVQEALDKAREGRTCIVIAHRLSTIQNADLIVVFQNGRVKEH
GTHQQLLAQKGIYFSMVSVQAGTQNL

Appendix B: Alignment of the protein sequences

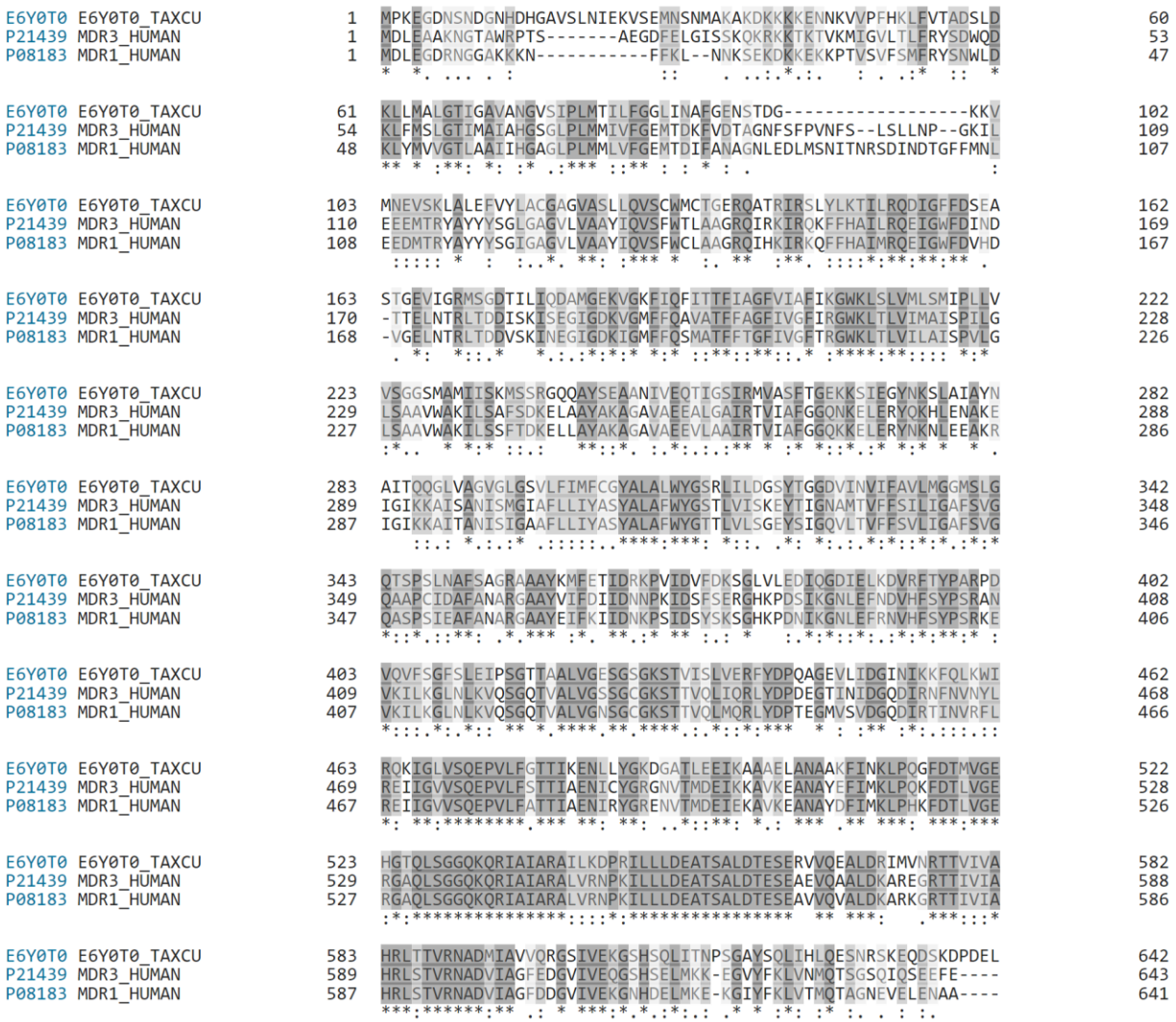
E6Y0T0 E6Y0T0_TAXCU 1 MPKEGDNSNDGNHDHGAVSLNIEKVSEMNSNMAKAKDKKKKENNKVVPFHKLFVTADSLD 60
P21439 MDR3_HUMAN 1 MDLEAAKNGTAWRPTS-------AEGDFELGISSKQKRKKTKTVKMIGVLTLFRYSDWQD 53
P08183 MDR1_HUMAN 1 MDLEGDRNGGAKKKN----------FFKL--NNKSEKDKKEKKPTVSVFSMFRYSNWLD 47
E6Y0T0 E6Y0T0_TAXCU 61 KLLMALGTIGAVANGVSIPLMTILFGGLINAFGENSTDG-----------------KKV 102
P21439 MDR3_HUMAN 54 KLFMSLGTIMAIAHGSGLPLMMIVFGEMTDKFVDTAGNFSFPVNFS--LSLLNP--GKIL 109
P08183 MDR1_HUMAN 48 KLYMVVGTLAAIIHGAGLPLMMLVFGEMTDIFANAGNLEDLMSNITNRSDINDTGFFMNL 107
E6Y0T0 E6Y0T0_TAXCU 103 MNEVSKLALEFVYLACGAGVASLLQVSCWMCTGERQATRIRSLYLKTILRQDIGFFDSEA 162
P21439 MDR3_HUMAN 110 EEEMTRYAYYYSGLGAGVLVAAYIQVSFWTLAAGRQIRKIRQKFFHAILRQEIGWFDIND 169
P08183 MDR1_HUMAN 108 EEDMTRYAYYYSGIGAGVLVAAYIQVSFWCLAAGRQIHKIRKQFFHAIMRQEIGWFDVHD 167
E6Y0T0 E6Y0T0_TAXCU 163 STGEVIGRMSGDTILIQDAMGEKVGKFIQFITTFIAGFVIAFIKGWKLSLVMLSMIPLLV 222
P21439 MDR3_HUMAN 170 -TTELNTRLTDDISKISEGIGDKVGMFFQAVATFFAGFIVGFIRGWKLTLVIMAISPILG 228
P08183 MDR1_HUMAN 168 -VGELNTRLTDDVSKINEGIGDKIGMFFQSMATFFTGFIVGFTRGWKLTLVILAISPVLG 226
E6Y0T0 E6Y0T0_TAXCU 223 VSGGSMAMIISKMSSRGQQAYSEAANIVEQTIGSIRMVASFTGEKKSIEGYNKSLAIAYN 282
P21439 MDR3_HUMAN 229 LSAAVWAKILSAFSDKELAAYAKAGAVAEEALGAIRTVIAFGGQNKELERYQKHLENAKE 288
P08183 MDR1_HUMAN 227 LSAAVWAKILSSFTDKELLAYAKAGAVAEEVLAAIRTVIAFGGQKKELERYNKNLEEAKR 286
E6Y0T0 E6Y0T0_TAXCU 283 AITQQGLVAGVGLGSVLFIMFCGYALALWYGSRLILDGSYTGGDVINVIFAVLMGGMSLG 342
P21439 MDR3_HUMAN 289 IGIKKAISANISMGIAFLLIYASYALAFWYGSTLVISKEYTIGNAMTVFFSILIGAFSVG 348
P08183 MDR1_HUMAN 287 IGIKKAITANISIGAAFLLIYASYALAFWYGTTLVLSGEYSIGQVLTVFFSVLIGAFSVG 346
E6Y0T0 E6Y0T0_TAXCU 343 QTSPSLNAFSAGRAAAYKMFETIDRKPVIDVFDKSGLVLEDIQGDIELKDVRFTYPARPD 402
P21439 MDR3_HUMAN 349 QAAPCIDAFANARGAAYVIFDIIDNNPKIDSFSERGHKPDSIKGNLEFNDVHFSYPSRAN 408
P08183 MDR1_HUMAN 347 QASPSIEAFANARGAAYEIFKIIDNKPSIDSYSKSGHKPDNIKGNLEFRNVHFSYPSRKE 406
E6Y0T0 E6Y0T0_TAXCU 403 VQVFSGFSLEIPSGTTAALVGESGSGKSTVISLVERFYDPQAGEVLIDGINIKKFQLKWI 462
P21439 MDR3_HUMAN 409 VKILKGLNLKVQSGQTVALVGSSGCGKSTTVQLIQRLYDPDEGTINIDGQDIRNFNVNYL 468
P08183 MDR1_HUMAN 407 VKILKGLNLKVQSGQTVALVGNSGCGKSTTVQLMQRLYDPTEGMVSVDGQDIRTINVRFL 466
E6Y0T0 E6Y0T0_TAXCU 463 RQKIGLVSQEPVLFGTTIKENLLYGKDGATLEEIKAAAELANAAKFINKLPQGFDTMVGE 522
P21439 MDR3_HUMAN 469 REIIGVVSQEPVLFSTTIAENICYGRGNVTMDEIKKAVKEANAYEFIMKLPQKFDTLVGE 528
P08183 MDR1_HUMAN 467 REIIGVVSQEPVLFATTIAENIRYGRENVTMDEIEKAVKEANAYDFIMKLPHKFDTLVGE 526
E6Y0T0 E6Y0T0_TAXCU 523 HGTQLSGGQKQRIAIARAILKDPRILLLDEATSALDTESERVVQEALDRIMVNRTTVIVA 582
P21439 MDR3_HUMAN 529 RGAQLSGGQKQRIAIARALVRNPKILLLDEATSALDTESEAEVQAALDKAREGRTTIVIA 588
P08183 MDR1_HUMAN 527 RGAQLSGGQKQRIAIARALVRNPKILLLDEATSALDTESEAVVQVALDKARKGRTTIVIA 586
E6Y0T0 E6Y0T0_TAXCU 583 HRLTTVRNADMIAVVQRGSIVEKGSHSQLITNPSGAYSQLIHLQESNRSKEQDSKDPDEL 642
P21439 MDR3_HUMAN 589 HRLSTVRNADVIAGFEDGVIVEQGSHSELMKK-EGVYFKLVNMQTSGSQIQSEEFE---- 643
P08183 MDR1_HUMAN 587 HRLSTVRNADVIAGFDDGVIVEKGNHDELMKE-KGIYFKLVTMQTAGNEVELENAA---- 641

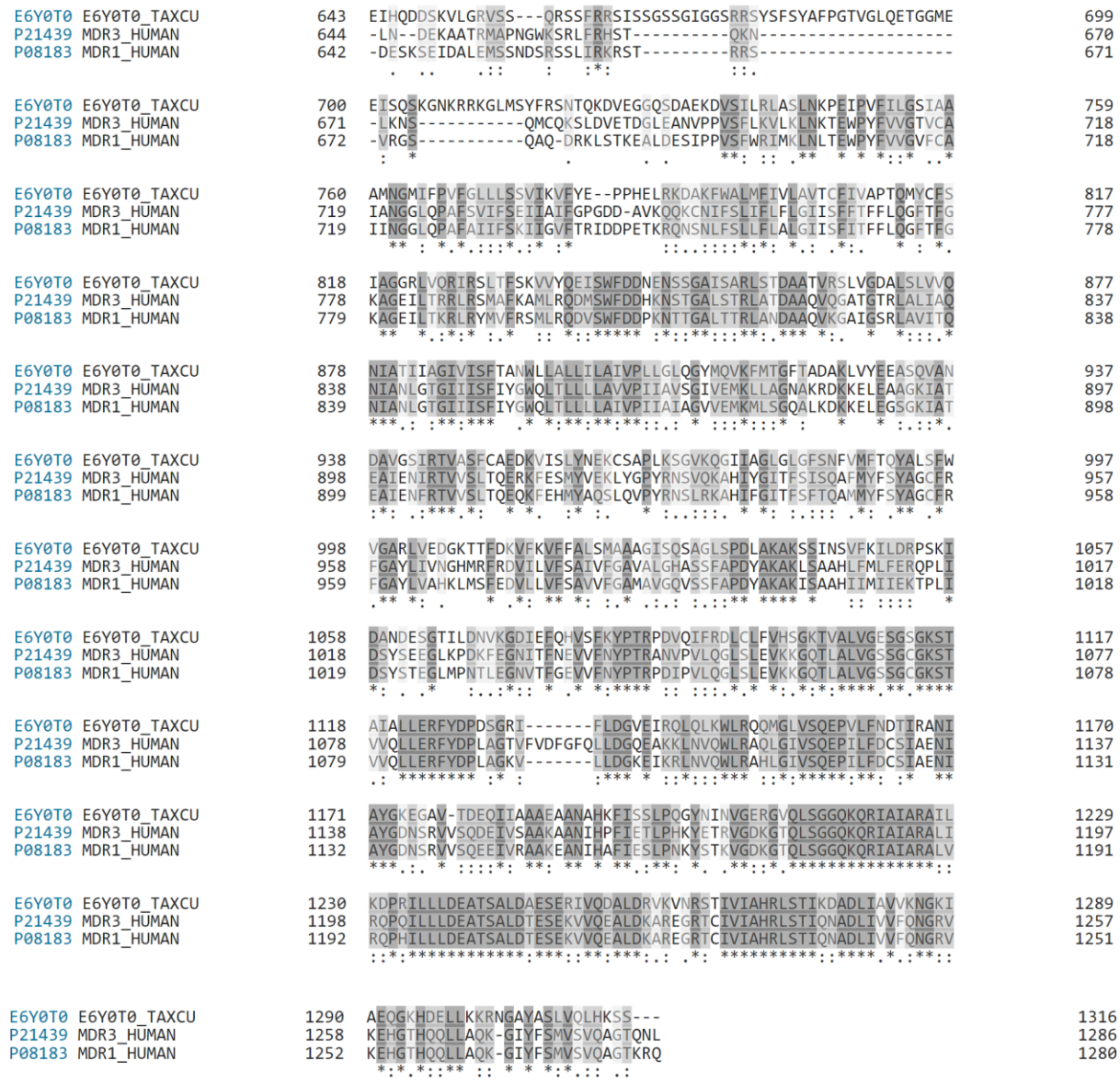

Appendix C: mRNA sequence of E6Y0T0

>ENA|DQ660357|DQ660357.1 Taxus cuspidata MDR-like ABC transporter (mdr) mRNA, complete cds.

GAGGCTGTCCTCATCTGCTGCGTTTTTGCAGAAAGAGTTTGGCCATTTTTTCTGTAGAAA
CTGATTCTTTCGGAGAAGTATTCGAGGAACATTGAATTTTCACTTGGAAATATTGACAGA
AATAGTGACTTTCGCCGATAATTTTTGATCTTTTCAACGAAGCTGGTGGAAGACTGACTT
TTAGATTGTTGCAGTGTTTTACGAGCAATTGCGTACAGACTTCGTCGAAATCTTTGCAGG
GGTGTTGAATAACTGATTATTCCCATTGGAGTGCCACAGTTTTCTCAAGGGAGTAGTTCC
ATCCCTGAAATCCGATATGCCAAAGGAAGGTGACAATTCCAATGATGGTAATCATGACCA
TGGTGCAGTATCTTTGAACATTGAGAAGGTTTCTGAAATGAACTCAAACATGGCTAAGGC
AAAGGACAAGAAAAAAAAAGAGAACAATAAGGTCGTGCCATTTCACAAATTATTTGTCAC
GGCAGACTCTCTGGATAAATTGTTGATGGCTCTTGGTACTATTGGTGCTGTGGCCAACGG
CGTATCTATTCCACTTATGACCATCCTGTTTGGGGGCCTTATAAATGCATTCGGGGAGAA
CAGCACAGACGGGAAAAAAGTGATGAATGAAGTGTCCAAGCTGGCTTTGGAGTTTGTTTA
TCTTGCCTGTGGTGCAGGAGTTGCAAGTTTACTTCAGGTGTCATGTTGGATGTGCACTGG

GGAAAGACAAGCTACACGCATCAGGAGTCTCTACCTAAAAACTATTTTGAGGCAAGATAT
TGGATTCTTTGATAGCGAGGCATCGACAGGAGAGGTTATTGGAAGGATGTCGGGCGACAC
CATATTAATTCAGGACGCCATGGGAGAAAAGGTTGGAAAGTTCATACAGTTCATAACCAC
ATTCATAGCAGGATTTGTTATAGCTTTCATCAAAGGTTGGAAACTTTCCCTGGTAATGCT
ATCCATGATTCCTCTTCTCGTTGTATCTGGCGGCTCGATGGCTATGATAATCTCCAAAAT
GTCAAGCCGAGGCCAGCAAGCTTATTCAGAAGCAGCCAATATTGTGGAGCAGACAATCGG
TTCAATTAGGATGGTTGCATCTTTTACTGGGGAAAAGAAATCCATAGAAGGTTATAACAA
GTCACTTGCGATAGCTTACAATGCTATCACTCAGCAAGGGTTGGTAGCTGGTGTTGGCCT
TGGGTCTGTTCTCTTTATCATGTTCTGTGGCTATGCATTGGCTCTTTGGTATGGATCACG
GTTAATTCTAGATGGAAGTTATACCGGTGGCGATGTGATCAATGTCATATTTGCAGTTCT
GATGGGAGGCATGTCTCTGGGCCAGACATCACCATCATTAAATGCTTTTTCAGCTGGACG
AGCTGCAGCATACAAAATGTTTGAGACTATTGACAGAAAACCAGTGATTGATGTCTTTGA
TAAATCTGGACTGGTCCTCGAGGATATTCAAGGTGATATTGAGCTTAAAGATGTACGGTT
CACGTATCCTGCTAGACCAGATGTTCAAGTCTTTTCTGGCTTTTCACTAGAAATACCTAG
CGGCACCACTGCAGCTTTAGTTGGAGAGAGTGGCAGTGGAAAGTCCACTGTTATCAGTCT
TGTAGAGAGATTCTATGATCCGCAAGCTGGCGAAGTGCTTATTGATGGCATTAACATCAA
GAAATTTCAGCTTAAGTGGATAAGGCAGAAAATTGGACTGGTGAGCCAGGAACCTGTTCT
TTTTGGTACCACCATTAAAGAGAACCTTTTATATGGTAAAGATGGAGCTACATTAGAGGA
AATCAAGGCTGCTGCTGAACTCGCCAATGCAGCAAAGTTTATAAACAAGTTGCCCCAGGG
TTTTGATACAATGGTGGGAGAGCATGGTACCCAACTATCTGGAGGTCAAAAACAAAGAAT
TGCAATTGCACGGGCTATTCTAAAAGATCCCCGAATTCTTCTCCTCGATGAAGCAACAAG
TGCATTGGATACAGAATCTGAAAGAGTTGTTCAAGAAGCCCTTGACAGGATTATGGTAAA
TAGAACAACAGTGATTGTTGCCCATCGTCTAACAACTGTCAGAAATGCTGACATGATTGC
TGTTGTCCAGCGTGGTTCAATTGTGGAAAAAGGTTCTCACTCTCAGCTTATCACAAACCC
TTCTGGTGCATACTCCCAGCTTATACATCTGCAAGAATCGAATCGATCAAAAGAACAAGA
TTCAAAGGATCCAGATGAATTGGAAATACATCAGGATGATAGCAAGGTTCTTGGTAGAGT
TAGCAGTCAAAGGTCATCTTTTAGACGGTCCATAAGCAGTGGATCATCAGGAATTGGTGG
AAGTCGTCGTTCATATTCATTTTCTTATGCTTTTCCTGGTACAGTAGGCCTCCAGGAAAC
TGGAGGTATGGAGGAAATCAGCCAATCAAAGGGAAACAAAAGAAGGAAGGGCCTGATGAG
TTATTTTAGGTCCAATACTCAGAAAGATGTGGAAGGTGGTCAATCTGATGCTGAGAAAGA
TGTTTCTATTTTACGTCTAGCATCTCTAAATAAGCCAGAGATTCCAGTGTTCATACTTGG
ATCAATTGCAGCAGCTATGAATGGGATGATATTTCCCGTCTTTGGTCTCTTGCTTTCAAG
TGTTATCAAGGTCTTCTATGAACCCCCTCATGAACTTCGAAAAGATGCCAAATTCTGGGC
ACTTATGTTTATAGTTTTGGCAGTTACGTGCTTCATTGTGGCACCTACACAGATGTATTG
TTTTTCCATAGCCGGTGGCAGGCTAGTGCAACGTATTCGATCGTTGACATTTTCCAAAGT
AGTTTACCAGGAGATTAGCTGGTTTGATGACAATGAAAACTCAAGCGGTGCAATAAGTGC
AAGATTATCAACAGATGCTGCAACTGTGCGTAGTTTGGTGGGAGATGCACTGTCACTTGT
TGTTCAAAATATAGCAACCATCATTGCTGGCATTGTCATATCTTTTACGGCCAACTGGTT
GCTAGCGCTTTTGATACTAGCTATAGTACCTCTTCTAGGTCTTCAAGGGTACATGCAAGT
AAAGTTCATGACGGGTTTCACTGCTGATGCAAAGTTGGTGTATGAGGAAGCCAGTCAAGT
TGCAAATGATGCTGTTGGAAGTATTCGAACTGTCGCCTCCTTCTGTGCAGAGGATAAGGT
TATCAGTCTCTACAATGAAAAATGCTCTGCTCCCTTGAAAAGTGGAGTTAAACAGGGAAT
TATAGCTGGACTTGGTTTAGGATTCTCAAATTTTGTGATGTTTACTCAATATGCACTCAG
CTTTTGGGTAGGGGCTCGCTTGGTTGAAGACGGAAAGACAACTTTTGATAAAGTTTTCAA
GGTGTTTTTTGCCCTCTCAATGGCTGCCGCGGGAATCTCTCAATCAGCAGGCCTTTCCCC
TGACCTTGCAAAAGCCAAGTCCTCTATCAATTCAGTGTTCAAAATTCTTGACCGTCCTTC
CAAGATCGACGCAAATGACGAGTCTGGGACTATCTTAGATAATGTGAAGGGTGACATTGA
GTTTCAGCATGTCAGCTTTAAATATCCAACTCGTCCAGATGTGCAAATCTTCCGTGATCT
ATGTTTATTTGTCCATTCTGGGAAGACTGTTGCTCTTGTGGGAGAGAGCGGAAGTGGTAA
ATCAACAGCCATTGCTCTTTTGGAGCGATTCTATGATCCTGATTCAGGCCGTATATTCCT
TGATGGAGTTGAAATTCGTCAACTTCAACTTAAATGGTTGCGACAACAGATGGGCTTGGT
GAGCCAAGAGCCTGTTTTGTTCAATGATACAATCCGTGCAAATATTGCTTATGGAAAGGA
GGGTGCAGTTACTGATGAGCAAATCATAGCAGCTGCTGAGGCTGCCAATGCCCACAAGTT
CATATCAAGCCTTCCCCAAGGATACAACATAAATGTTGGCGAGCGAGGGGTGCAATTATC
TGGGGGTCAAAAGCAACGCATTGCAATCGCAAGAGCAATACTAAAAGATCCCAGGATACT
TCTCTTGGATGAAGCTACAAGTGCCCTAGATGCTGAATCAGAGCGCATAGTTCAAGATGC
ATTGGACCGTGTAAAGGTAAACAGGTCTACTATTGTCATTGCTCACCGTCTTTCAACAAT

TAAAGATGCAGATCTCATAGCAGTGGTGAAGAATGGAAAAATTGCAGAACAAGGAAAGCA
TGATGAATTGCTGAAGAAGCGAAATGGAGCCTATGCATCCCTAGTGCAATTGCATAAGTC
CTCATAGTTTATTTTTCTGGAAATACAGAAATTTGTCTAGTGTGTATTTCATGCACATTG
CTAGTAAAAAAATACTGGCAGGCAACAAAGTTAAGTTGCTATTGGTATCTTTCTAGGTCC
ATAATATACAGTTGAAACAGCCAACAAAATGAATTGCTGTACTTTTATGTGGGAATAAAT
TATTTAATTTGGGGACCAAAAAAAAAAAAAAAAAAAAAAAAAA

Appendix D: Statistic analysis results

Two-way Anova test results

Results of media samples with verapamil treatment

Two-way RM ANOVA	Matching: Stacked				
Alpha	0.05				
Source of Variation	% of total variation	P value	P value summary	Significant?	
Interaction	7.856	0.0955	ns	No	
Time	63.49	<0.0001	****	Yes	
Verapamil	13.81	0.0110	*	Yes	
Subjects (matching)	3.946	0.4069	ns	No	
ANOVA table	SS	DF	MS	F (DFn, DFd)	P value
Interaction	0.5364	6	0.08941	F (6, 18) = 2.164	P=0.0955
Time	4.336	3	1.445	F (3, 18) = 34.98	P<0.0001
Verapamil	0.9431	2	0.4716	F (2, 6) = 10.5	P=0.0110
Subjects (matching)	0.2695	6	0.04491	F (6, 18) = 1.087	P=0.4069
Residual	0.7437	18	0.04132		

Results of media samples with genistein treatment

Two-way RM ANOVA	Matching: Stacked				
Alpha	0.05				
Source of Variation	% of total variation	P value	P value summary	Significant?	
Interaction	11.35	0.0512	ns	No	
Time	54.06	<0.0001	****	Yes	
Genistein	13.08	0.0627	ns	No	
Subjects (matching)	8.625	0.1175	ns	No	
ANOVA table	SS	DF	MS	F (DFn, DFd)	P value
Interaction	0.5758	6	0.09597	F (6, 18) = 2.643	P=0.0512
Time	2.743	3	0.9144	F (3, 18) = 25.18	P<0.0001
Genistein	0.6639	2	0.3319	F (2, 6) = 4.551	P=0.0627
Subjects (matching)	0.4376	6	0.07294	F (6, 18) = 2.009	P=0.1175
Residual	0.6536	18	0.03631		

Results of media samples with cyclosporine A treatment

Two-way RM ANOVA	Matching: Stacked				
Alpha	0.05				
Source of Variation	% of total variation	P value	P value summary	Significant?	
Interaction	20.24	<0.0001	****	Yes	
Time	35.27	<0.0001	****	Yes	
Cyclosporine A	33.07	0.0029	**	Yes	
Subjects (matching)	5.486	0.0434	*	Yes	
ANOVA table	SS	DF	MS	F (DFn, DFd)	P value
Interaction	1.692	6	0.2819	F (6, 18) = 10.23	P<0.0001
Time	2.948	3	0.9827	F (3, 18) = 35.66	P<0.0001
Cyclosporine A	2.764	2	1.382	F (2, 6) = 18.08	P=0.0029
Subjects (matching)	0.4586	6	0.07643	F (6, 18) = 2.773	P=0.0434
Residual	0.496	18	0.02756		

Results of media samples with vanadate treatment

Two-way RM ANOVA	Matching: Stacked				
Alpha	0.05				
Source of Variation	% of total variation	P value	P value summary	Significant?	
Interaction	8.931	0.2102	ns	No	
Time	49.73	<0.0001	****	Yes	
Vanadae	16.08	0.0393	*	Yes	
Subjects (matching)	8.288	0.2454	ns	No	
ANOVA table	SS	DF	MS	F (DFn, DFd)	P value
Interaction	0.4487	6	0.07478	F (6, 18) = 1.579	P=0.2102
Time	2.498	3	0.8328	F (3, 18) = 17.59	P<0.0001
Vanadae	0.8078	2	0.4039	F (2, 6) = 5.82	P=0.0393
Subjects (matching)	0.4164	6	0.06939	F (6, 18) = 1.465	P=0.2454
Residual	0.8524	18	0.04736		

Results of cell samples with verapamil treatment

Two-way RM ANOVA	Matching: Stacked				
Alpha	0.05				
Source of Variation	% of total variation	P value	P value summary	Significant?	
Interaction	25.87	0.0043	**	Yes	
Time	45.37	<0.0001	****	Yes	
Column Factor	1.172	0.7470	ns	No	
Subjects (matching)	11.48	0.0991	ns	No	
ANOVA table	SS	DF	MS	F (DFn, DFd)	P value
Interaction	0.1911	6	0.03185	F (6, 18) = 4.816	P=0.0043
Time	0.3352	3	0.1117	F (3, 18) = 16.9	P<0.0001
Column Factor	0.008656	2	0.004328	F (2, 6) = 0.3063	P=0.7470
Subjects (matching)	0.08477	6	0.01413	F (6, 18) = 2.137	P=0.0991
Residual	0.119	18	0.006613		

Results of cell samples with genistein treatment

Two-way RM ANOVA	Matching: Stacked				
Alpha	0.05				
Source of Variation	% of total variation	P value	P value summary	Significant?	
Interaction	21.61	0.0268	*	Yes	
Time	43.19	0.0001	***	Yes	
Genistein	3.553	0.4362	ns	No	
Subjects (matching)	11.15	0.1955	ns	No	
ANOVA table	SS	DF	MS	F (DFn, DFd)	P value
Interaction	0.1161	6	0.01935	F (6, 18) = 3.162	P=0.0268
Time	0.2321	3	0.07737	F (3, 18) = 12.64	P=0.0001
Genistein	0.0191	2	0.009549	F (2, 6) = 0.9557	P=0.4362
Subjects (matching)	0.05995	6	0.009992	F (6, 18) = 1.632	P=0.1955
Residual	0.1102	18	0.006121		

Results of cell samples with cyclosporine A treatment

Two-way RM ANOVA	Matching: Stacked				
Alpha	0.05				
Source of Variation	% of total variation	P value	P value summary	Significant?	
Interaction	4.994	0.7359	ns	No	
Time	51.49	0.0001	***	Yes	
Column Factor	0.7763	0.8762	ns	No	
Subjects (matching)	17.24	0.1143	ns	No	
ANOVA table	SS	DF	MS	F (DFn, DFd)	P value
Interaction	0.02527	6	0.004211	F (6, 18) = 0.5877	P=0.7359
Time	0.2605	3	0.08685	F (3, 18) = 12.12	P=0.0001
Column Factor	0.003928	2	0.001964	F (2, 6) = 0.1351	P=0.8762
Subjects (matching)	0.08725	6	0.01454	F (6, 18) = 2.029	P=0.1143
Residual	0.129	18	0.007166		

Results of cell samples with vanadate treatment

Two-way RM ANOVA	Matching: Stacked				
Alpha	0.05				
Source of Variation	% of total variation	P value	P value summary	Significant?	
Interaction	7.722	0.5247	ns	No	
Time	48.47	0.0002	***	Yes	
Column Factor	8.333	0.1479	ns	No	
Subjects (matching)	9.352	0.4139	ns	No	
ANOVA table	SS	DF	MS	F (DFn, DFd)	P value
Interaction	0.05773	6	0.009622	F (6, 18) = 0.8867	P=0.5247
Time	0.3624	3	0.1208	F (3, 18) = 11.13	P=0.0002
Column Factor	0.0623	2	0.03115	F (2, 6) = 2.673	P=0.1479
Subjects (matching)	0.06992	6	0.01165	F (6, 18) = 1.074	P=0.4139
Residual	0.1953	18	0.01085		

Tukey's multiple comparison results

Results of media samples with verapamil treatment

Tukey's multiple compariso	Mean Diff.	95.00% CI of diff.	Significant?	Summary	Adjusted P Value
1.5h					
V-50 vs. V-100	-0.1676	-0.5866 to 0.2513	No	ns	0.5845
V-50 vs. Control	-0.3456	-0.7646 to 0.07333	No	ns	0.1197
V-100 vs. Control	-0.178	-0.5969 to 0.241	No	ns	0.5468
3h					
V-50 vs. V-100	0.296	-0.1229 to 0.715	No	ns	0.2028
V-50 vs. Control	-0.06618	-0.4851 to 0.3528	No	ns	0.9181
V-100 vs. Control	-0.3622	-0.7812 to 0.05674	No	ns	0.0991
6h					
V-50 vs. V-100	0.5904	0.1714 to 1.009	Yes	**	0.0048
V-50 vs. Control	-0.07291	-0.4919 to 0.346	No	ns	0.9015
V-100 vs. Control	-0.6633	-1.082 to -0.2444	Yes	**	0.0017
24h					
V-50 vs. V-100	0.008713	-0.4102 to 0.4277	No	ns	0.9985
V-50 vs. Control	-0.3719	-0.7909 to 0.04704	No	ns	0.0886
V-100 vs. Control	-0.3806	-0.7996 to 0.03833	No	ns	0.0799

Test details	Mean 1	Mean 2	Mean Diff.	SE of diff.	N1	N2	q	DF
1.5h								
V-50 vs. V-100	1.68	1.848	-0.1676	0.1678	3	3	1.413	24
V-50 vs. Control	1.68	2.026	-0.3456	0.1678	3	3	2.914	24
V-100 vs. Control	1.848	2.026	-0.178	0.1678	3	3	1.5	24
3h								
V-50 vs. V-100	1.643	1.347	0.296	0.1678	3	3	2.495	24
V-50 vs. Control	1.643	1.709	-0.06618	0.1678	3	3	0.5579	24
V-100 vs. Control	1.347	1.709	-0.3622	0.1678	3	3	3.053	24
6h								
V-50 vs. V-100	1.55	0.9594	0.5904	0.1678	3	3	4.977	24
V-50 vs. Control	1.55	1.623	-0.07291	0.1678	3	3	0.6146	24
V-100 vs. Control	0.9594	1.623	-0.6633	0.1678	3	3	5.592	24
24h								
V-50 vs. V-100	0.7769	0.7681	0.008713	0.1678	3	3	0.07345	24
V-50 vs. Control	0.7769	1.149	-0.3719	0.1678	3	3	3.135	24
V-100 vs. Control	0.7681	1.149	-0.3806	0.1678	3	3	3.209	24

Results of media samples with genistein treatment

Tukey's multiple comparisons test	Mean Diff.	95.00% CI of diff.	Significant?	Summary	Adjusted P Value
1.5h					
Control vs. G-50	0.1211	-0.3136 to 0.5559	No	ns	0.7682
Control vs. G-100	0.2539	-0.1808 to 0.6887	No	ns	0.3281
G-50 vs. G-100	0.1328	-0.302 to 0.5676	No	ns	0.7289
3h					
Control vs. G-50	-0.00419	-0.439 to 0.4306	No	ns	0.9997
Control vs. G-100	0.1205	-0.3143 to 0.5552	No	ns	0.7704
G-50 vs. G-100	0.1246	-0.3101 to 0.5594	No	ns	0.7565
6h					
Control vs. G-50	0.09149	-0.3433 to 0.5263	No	ns	0.8597
Control vs. G-100	0.7615	0.3267 to 1.196	Yes	***	0.0006
G-50 vs. G-100	0.67	0.2353 to 1.105	Yes	**	0.0021
24h					
Control vs. G-50	-0.1764	-0.6112 to 0.2584	No	ns	0.5759
Control vs. G-100	0.03207	-0.4027 to 0.4668	No	ns	0.9815
G-50 vs. G-100	0.2085	-0.2263 to 0.6432	No	ns	0.4662

Test details	Mean 1	Mean 2	Mean Diff.	SE of diff.	N1	N2	q	DF
1.5h								
Control vs. G-50	2.026	1.905	0.1211	0.1741	3	3	0.9839	24
Control vs. G-100	2.026	1.772	0.2539	0.1741	3	3	2.063	24
G-50 vs. G-100	1.905	1.772	0.1328	0.1741	3	3	1.079	24
3h								
Control vs. G-50	1.709	1.713	-0.00419	0.1741	3	3	0.03404	24
Control vs. G-100	1.709	1.588	0.1205	0.1741	3	3	0.9785	24
G-50 vs. G-100	1.713	1.588	0.1246	0.1741	3	3	1.013	24
6h								
Control vs. G-50	1.623	1.531	0.09149	0.1741	3	3	0.7432	24
Control vs. G-100	1.623	0.8612	0.7615	0.1741	3	3	6.186	24
G-50 vs. G-100	1.531	0.8612	0.67	0.1741	3	3	5.443	24
24h								
Control vs. G-50	1.149	1.325	-0.1764	0.1741	3	3	1.433	24
Control vs. G-100	1.149	1.117	0.03207	0.1741	3	3	0.2605	24
G-50 vs. G-100	1.325	1.117	0.2085	0.1741	3	3	1.693	24

Results of media samples with cyclosporine A treatment

Tukey's multiple comparisons test	Mean Diff.	95.00% CI of diff.	Significant?	Summary	Adjusted P Value
1.5h					
Control vs. CA-50	0.003464	-0.4032 to 0.4101	No	ns	0.9998
Control vs. CA-100	1.138	0.7312 to 1.545	Yes	****	<0.0001
CA-50 vs. CA-100	1.134	0.7278 to 1.541	Yes	****	<0.0001
3h					
Control vs. CA-50	-0.1415	-0.5482 to 0.2652	No	ns	0.6646
Control vs. CA-100	0.02194	-0.3847 to 0.4286	No	ns	0.9900
CA-50 vs. CA-100	0.1634	-0.2432 to 0.5701	No	ns	0.5817
6h					
Control vs. CA-50	-0.01559	-0.4222 to 0.3911	No	ns	0.9950
Control vs. CA-100	0.9216	0.5149 to 1.328	Yes	****	<0.0001
CA-50 vs. CA-100	0.9371	0.5305 to 1.344	Yes	****	<0.0001
24h					
Control vs. CA-50	0.1281	-0.2786 to 0.5347	No	ns	0.7148
Control vs. CA-100	0.257	-0.1497 to 0.6636	No	ns	0.2742
CA-50 vs. CA-100	0.1289	-0.2778 to 0.5356	No	ns	0.7117

Test details	Mean 1	Mean 2	Mean Diff.	SE of diff.	N1	N2	q	DF
1.5h								
Control vs. CA-50	2.026	2.022	0.003464	0.1628	3	3	0.03008	24
Control vs. CA-100	2.026	0.888	1.138	0.1628	3	3	9.882	24
CA-50 vs. CA-100	2.022	0.888	1.134	0.1628	3	3	9.852	24
3h								
Control vs. CA-50	1.709	1.85	-0.1415	0.1628	3	3	1.229	24
Control vs. CA-100	1.709	1.687	0.02194	0.1628	3	3	0.1905	24
CA-50 vs. CA-100	1.85	1.687	0.1634	0.1628	3	3	1.419	24
6h								
Control vs. CA-50	1.623	1.638	-0.01559	0.1628	3	3	0.1354	24
Control vs. CA-100	1.623	0.7012	0.9216	0.1628	3	3	8.003	24
CA-50 vs. CA-100	1.638	0.7012	0.9371	0.1628	3	3	8.139	24
24h								
Control vs. CA-50	1.149	1.021	0.1281	0.1628	3	3	1.112	24
Control vs. CA-100	1.149	0.8918	0.257	0.1628	3	3	2.232	24
CA-50 vs. CA-100	1.021	0.8918	0.1289	0.1628	3	3	1.12	24

Results of media samples with vanadate treatment

Tukey's multiple comparisons test	Mean Diff.	95.00% CI of diff.	Significant?	Summary	Adjusted P Value
1.5h					
Control vs. VA-50	0.07481	-0.394 to 0.5436	No	ns	0.9165
Control vs. VA-100	0.6758	0.207 to 1.145	Yes	**	0.0040
VA-50 vs. VA-100	0.601	0.1322 to 1.07	Yes	*	0.0103
3h					
Control vs. VA-50	0.2498	-0.219 to 0.7186	No	ns	0.3926
Control vs. VA-100	0.3365	-0.1323 to 0.8053	No	ns	0.1935
VA-50 vs. VA-100	0.08672	-0.3821 to 0.5555	No	ns	0.8896
6h					
Control vs. VA-50	0.1171	-0.3517 to 0.5859	No	ns	0.8087
Control vs. VA-100	0.3426	-0.1262 to 0.8114	No	ns	0.1830
VA-50 vs. VA-100	0.2255	-0.2433 to 0.6943	No	ns	0.4639
24h					
Control vs. VA-50	0.2127	-0.2561 to 0.6815	No	ns	0.5037
Control vs. VA-100	0.11	-0.3588 to 0.5789	No	ns	0.8288
VA-50 vs. VA-100	-0.1027	-0.5715 to 0.3661	No	ns	0.8490

Test details	Mean 1	Mean 2	Mean Diff.	SE of diff.	N1	N2	q	DF
1.5h								
Control vs. VA-50	2.026	1.951	0.07481	0.1877	3	3	0.5636	24
Control vs. VA-100	2.026	1.35	0.6758	0.1877	3	3	5.091	24
VA-50 vs. VA-100	1.951	1.35	0.601	0.1877	3	3	4.527	24
3h								
Control vs. VA-50	1.709	1.459	0.2498	0.1877	3	3	1.882	24
Control vs. VA-100	1.709	1.372	0.3365	0.1877	3	3	2.535	24
VA-50 vs. VA-100	1.459	1.372	0.08672	0.1877	3	3	0.6533	24
6h								
Control vs. VA-50	1.623	1.506	0.1171	0.1877	3	3	0.882	24
Control vs. VA-100	1.623	1.28	0.3426	0.1877	3	3	2.581	24
VA-50 vs. VA-100	1.506	1.28	0.2255	0.1877	3	3	1.699	24
24h								
Control vs. VA-50	1.149	0.9361	0.2127	0.1877	3	3	1.602	24
Control vs. VA-100	1.149	1.039	0.11	0.1877	3	3	0.8289	24
VA-50 vs. VA-100	0.9361	1.039	-0.1027	0.1877	3	3	0.7735	24

Results of cell samples with verapamil treatment

Tukey's multiple comparisons test	Mean Diff.	95.00% CI of diff.	Significant?	Summary	Adjusted P Value
1.5h					
V-50 vs. V-100	-0.06826	-0.2562 to 0.1196	No	ns	0.6411
V-50 vs. Control	0.06252	-0.1254 to 0.2504	No	ns	0.6879
V-100 vs. Control	0.1308	-0.05713 to 0.3187	No	ns	0.2120
3h					
V-50 vs. V-100	-0.02079	-0.2087 to 0.1671	No	ns	0.9588
V-50 vs. Control	-0.2804	-0.4683 to -0.09252	Yes	**	0.0029
V-100 vs. Control	-0.2596	-0.4475 to -0.07173	Yes	**	0.0057
6h					
V-50 vs. V-100	-0.05715	-0.2451 to 0.1308	No	ns	0.7309
V-50 vs. Control	0.03373	-0.1542 to 0.2216	No	ns	0.8956
V-100 vs. Control	0.09088	-0.09702 to 0.2788	No	ns	0.4601
24h					
V-50 vs. V-100	-0.003017	-0.1909 to 0.1849	No	ns	0.9991
V-50 vs. Control	0.08485	-0.1031 to 0.2727	No	ns	0.5068
V-100 vs. Control	0.08786	-0.1 to 0.2758	No	ns	0.4833

Test details	Mean 1	Mean 2	Mean Diff.	SE of diff.	N1	N2	q	DF
1.5h								
V-50 vs. V-100	0.2157	0.2839	-0.06826	0.07524	3	3	1.283	24
V-50 vs. Control	0.2157	0.1531	0.06252	0.07524	3	3	1.175	24
V-100 vs. Control	0.2839	0.1531	0.1308	0.07524	3	3	2.458	24
3h								
V-50 vs. V-100	0.08909	0.1099	-0.02079	0.07524	3	3	0.3908	24
V-50 vs. Control	0.08909	0.3695	-0.2804	0.07524	3	3	5.271	24
V-100 vs. Control	0.1099	0.3695	-0.2596	0.07524	3	3	4.88	24
6h								
V-50 vs. V-100	0.4023	0.4595	-0.05715	0.07524	3	3	1.074	24
V-50 vs. Control	0.4023	0.3686	0.03373	0.07524	3	3	0.634	24
V-100 vs. Control	0.4595	0.3686	0.09088	0.07524	3	3	1.708	24
24h								
V-50 vs. V-100	0.4055	0.4085	-0.003017	0.07524	3	3	0.05671	24
V-50 vs. Control	0.4055	0.3207	0.08485	0.07524	3	3	1.595	24
V-100 vs. Control	0.4085	0.3207	0.08786	0.07524	3	3	1.651	24

Results of cell samples with genistein treatment

Tukey's multiple comparisons test	Mean Diff.	95.00% CI of diff.	Significant?	Summary	Adjusted P Value
1.5h					
Control vs. G-50	-0.05675	-0.2284 to 0.1149	No	ns	0.6911
Control vs. G-100	0.007534	-0.1641 to 0.1792	No	ns	0.9934
G-50 vs. G-100	0.06428	-0.1074 to 0.236	No	ns	0.6239
3h					
Control vs. G-50	0.2506	0.07894 to 0.4223	Yes	**	0.0035
Control vs. G-100	0.1168	-0.0549 to 0.2884	No	ns	0.2263
G-50 vs. G-100	-0.1338	-0.3055 to 0.03783	No	ns	0.1475
6h					
Control vs. G-50	0.09278	-0.07889 to 0.2645	No	ns	0.3825
Control vs. G-100	-0.01992	-0.1916 to 0.1517	No	ns	0.9549
G-50 vs. G-100	-0.1127	-0.2844 to 0.05897	No	ns	0.2490
24h					
Control vs. G-50	-0.07819	-0.2499 to 0.09348	No	ns	0.5011
Control vs. G-100	-0.07502	-0.2467 to 0.09665	No	ns	0.5285
G-50 vs. G-100	0.003167	-0.1685 to 0.1748	No	ns	0.9988

Test details	Mean 1	Mean 2	Mean Diff.	SE of diff.	N1	N2	q	DF
1.5h								
Control vs. G-50	0.1531	0.2099	-0.05675	0.06874	3	3	1.168	24
Control vs. G-100	0.1531	0.1456	0.007534	0.06874	3	3	0.155	24
G-50 vs. G-100	0.2099	0.1456	0.06428	0.06874	3	3	1.323	24
3h								
Control vs. G-50	0.3695	0.1189	0.2506	0.06874	3	3	5.156	24
Control vs. G-100	0.3695	0.2527	0.1168	0.06874	3	3	2.402	24
G-50 vs. G-100	0.1189	0.2527	-0.1338	0.06874	3	3	2.753	24
6h								
Control vs. G-50	0.3686	0.2758	0.09278	0.06874	3	3	1.909	24
Control vs. G-100	0.3686	0.3885	-0.01992	0.06874	3	3	0.4098	24
G-50 vs. G-100	0.2758	0.3885	-0.1127	0.06874	3	3	2.319	24
24h								
Control vs. G-50	0.3207	0.3988	-0.07819	0.06874	3	3	1.609	24
Control vs. G-100	0.3207	0.3957	-0.07502	0.06874	3	3	1.543	24
G-50 vs. G-100	0.3988	0.3957	0.003167	0.06874	3	3	0.06515	24

Results of cell samples with cyclosporine A treatment

Tukey's multiple comparisons test	Mean Diff.	95.00% CI of diff.	Significant?	Summary	Adjusted P Value
1.5h					
Control vs. CA-50	-0.02639	-0.2199 to 0.1672	No	ns	0.9383
Control vs. CA-100	-0.008942	-0.2025 to 0.1846	No	ns	0.9927
CA-50 vs. CA-100	0.01745	-0.1761 to 0.211	No	ns	0.9725
3h					
Control vs. CA-50	0.05862	-0.1349 to 0.2522	No	ns	0.7328
Control vs. CA-100	0.05038	-0.1432 to 0.2439	No	ns	0.7941
CA-50 vs. CA-100	-0.008238	-0.2018 to 0.1853	No	ns	0.9938
6h					
Control vs. CA-50	3.633e-005	-0.1935 to 0.1936	No	ns	>0.9999
Control vs. CA-100	0.0007593	-0.1928 to 0.1943	No	ns	>0.9999
CA-50 vs. CA-100	0.000723	-0.1928 to 0.1943	No	ns	>0.9999
24h					
Control vs. CA-50	-0.1188	-0.3123 to 0.07475	No	ns	0.2939
Control vs. CA-100	-0.03813	-0.2317 to 0.1554	No	ns	0.8758
CA-50 vs. CA-100	0.08067	-0.1129 to 0.2742	No	ns	0.5590

Test details	Mean 1	Mean 2	Mean Diff.	SE of diff.	N1	N2	q	DF
1.5h								
Control vs. CA-50	0.1531	0.1795	-0.02639	0.0775	3	3	0.4815	24
Control vs. CA-100	0.1531	0.1621	-0.008942	0.0775	3	3	0.1632	24
CA-50 vs. CA-100	0.1795	0.1621	0.01745	0.0775	3	3	0.3183	24
3h								
Control vs. CA-50	0.3695	0.3109	0.05862	0.0775	3	3	1.07	24
Control vs. CA-100	0.3695	0.3191	0.05038	0.0775	3	3	0.9193	24
CA-50 vs. CA-100	0.3109	0.3191	-0.008238	0.0775	3	3	0.1503	24
6h								
Control vs. CA-50	0.3686	0.3685	3.633e-005	0.0775	3	3	0.000663	24
Control vs. CA-100	0.3686	0.3678	0.0007593	0.0775	3	3	0.01386	24
CA-50 vs. CA-100	0.3685	0.3678	0.000723	0.0775	3	3	0.01319	24
24h								
Control vs. CA-50	0.3207	0.4394	-0.1188	0.0775	3	3	2.168	24
Control vs. CA-100	0.3207	0.3588	-0.03813	0.0775	3	3	0.6958	24
CA-50 vs. CA-100	0.4394	0.3588	0.08067	0.0775	3	3	1.472	24

Results of cell samples with vanadate treatment

Tukey's multiple comparisons test	Mean Diff.	95.00% CI of diff.	Significant?	Summary	Adjusted P Value
1.5h					
Control vs. VA-50	-0.08871	-0.3031 to 0.1256	No	ns	0.5635
Control vs. VA-100	-0.1057	-0.3201 to 0.1086	No	ns	0.4466
VA-50 vs. VA-100	-0.01701	-0.2314 to 0.1973	No	ns	0.9786
3h					
Control vs. VA-50	0.027	-0.1874 to 0.2414	No	ns	0.9471
Control vs. VA-100	0.03265	-0.1817 to 0.247	No	ns	0.9236
VA-50 vs. VA-100	0.00565	-0.2087 to 0.22	No	ns	0.9976
6h					
Control vs. VA-50	-0.2158	-0.4302 to -0.001443	Yes	*	0.0483
Control vs. VA-100	-0.1787	-0.3931 to 0.03566	No	ns	0.1149
VA-50 vs. VA-100	0.0371	-0.1773 to 0.2515	No	ns	0.9026
24h					
Control vs. VA-50	-0.06334	-0.2777 to 0.151	No	ns	0.7437
Control vs. VA-100	-0.1122	-0.3265 to 0.1022	No	ns	0.4051
VA-50 vs. VA-100	-0.04885	-0.2632 to 0.1655	No	ns	0.8377

Test details	Mean 1	Mean 2	Mean Diff.	SE of diff.	N1	N2	q	DF
1.5h								
Control vs. VA-50	0.1531	0.2419	-0.08871	0.08584	3	3	1.462	24
Control vs. VA-100	0.1531	0.2589	-0.1057	0.08584	3	3	1.742	24
VA-50 vs. VA-100	0.2419	0.2589	-0.01701	0.08584	3	3	0.2802	24
3h								
Control vs. VA-50	0.3695	0.3425	0.027	0.08584	3	3	0.4448	24
Control vs. VA-100	0.3695	0.3369	0.03265	0.08584	3	3	0.5379	24
VA-50 vs. VA-100	0.3425	0.3369	0.00565	0.08584	3	3	0.09309	24
6h								
Control vs. VA-50	0.3686	0.5844	-0.2158	0.08584	3	3	3.555	24
Control vs. VA-100	0.3686	0.5473	-0.1787	0.08584	3	3	2.944	24
VA-50 vs. VA-100	0.5844	0.5473	0.0371	0.08584	3	3	0.6112	24
24h								
Control vs. VA-50	0.3207	0.384	-0.06334	0.08584	3	3	1.044	24
Control vs. VA-100	0.3207	0.4328	-0.1122	0.08584	3	3	1.848	24
VA-50 vs. VA-100	0.384	0.4328	-0.04885	0.08584	3	3	0.8048	24

Student's t-test results

Results of the verapamil treated groups in preliminary inhibitor test

1.5h

t-Test: Two-Sample Assuming Unequal Variances

	V 50 uM	*control*
Mean	1.680299	2.025925
Variance	0.061311	0.0714
Observations	3	3
Hypothesized Mean Difference	0	
df	4	
t Stat	-1.64328	
P(T<=t) one-tail	0.087835	
t Critical one-tail	2.131847	
P(T<=t) two-tail	0.175669	
t Critical two-tail	2.776445	

t-Test: Two-Sample Assuming Unequal Variances

	V 100 uM	*control*
Mean	1.847929	2.025925
Variance	0.018364	0.0714
Observations	3	3
Hypothesized Mean Difference	0	
df	3	
t Stat	-1.029	
P(T<=t) one-tail	0.189591	
t Critical one-tail	2.353363	
P(T<=t) two-tail	0.379182	
t Critical two-tail	3.182446	

3h

t-Test: Two-Sample Assuming Unequal Variances

	V 50 uM	*control*
Mean	1.64253	1.70871
Variance	0.000185	0.020197
Observations	3	3
Hypothesized Mean Difference	0	
df	2	
t Stat	-0.8029	
P(T<=t) one-tail	0.253141	
t Critical one-tail	2.919986	
P(T<=t) two-tail	0.506282	
t Critical two-tail	4.302653	

t-Test: Two-Sample Assuming Unequal Variances

	V 100 uM	*control*
Mean	1.346502	1.70871
Variance	0.084073	0.020197
Observations	3	3
Hypothesized Mean Difference	0	
df	3	
t Stat	-1.94285	
P(T<=t) one-tail	0.07365	
t Critical one-tail	2.353363	
P(T<=t) two-tail	0.1473	
t Critical two-tail	3.182446	

6h

t-Test: Two-Sample Assuming Unequal Variances

	V 50 uM	*control*
Mean	1.54981	1.622723
Variance	0.031034	0.026359
Observations	3	3
Hypothesized Mean Difference	0	
df	4	
t Stat	-0.52715	
P(T<=t) one-tail	0.312986	
t Critical one-tail	2.131847	
P(T<=t) two-tail	0.625973	
t Critical two-tail	2.776445	

t-Test: Two-Sample Assuming Unequal Variances

	V 100 uM	*control*
Mean	0.959416	1.622723
Variance	0.086751	0.026359
Observations	3	3
Hypothesized Mean Difference	0	
df	3	
t Stat	-3.41605	
P(T<=t) one-tail	0.020982	
t Critical one-tail	2.353363	
P(T<=t) two-tail	0.041964	
t Critical two-tail	3.182446	

24h

t-Test: Two-Sample Assuming Unequal Variances

	V 50 uM	*control*
Mean	0.776851	1.14876
Variance	0.097829	0.008311
Observations	3	3
Hypothesized Mean Difference	0	
df	2	
t Stat	-1.97723	
P(T<=t) one-tail	0.093319	
t Critical one-tail	2.919986	
P(T<=t) two-tail	0.186638	
t Critical two-tail	4.302653	

t-Test: Two-Sample Assuming Unequal Variances

	V 100 uM	*control*
Mean	0.768139	1.14876
Variance	0.00078	0.008311
Observations	3	3
Hypothesized Mean Difference	0	
df	2	
t Stat	-6.91431	
P(T<=t) one-tail	0.010141	
t Critical one-tail	2.919986	
P(T<=t) two-tail	0.020283	
t Critical two-tail	4.302653	

Results of test with higher verapamil concentration after 24 hours incubation

t-Test: Two-Sample Assuming Unequal Variances		
	V	*comtrol*
Mean	41.44077	27.46144
Variance	4.678005	60.56909
Observations	3	3
Hypothesized Mean Difference	0	
df	2	
t Stat	2.99755	
P(T<=t) one-tail	0.0478	
t Critical one-tail	2.919986	
P(T<=t) two-tail	0.0956	
t Critical two-tail	4.302653	